Microchimica Acta (2022) 189: 94
https://doi.org/10.1007/s00604-022-05184-x

REVIEW ARTICLE

Electrochemical nanobiosensors equipped with peptides: a review

Masoud Negahdary[1] · **Lúcio Angnes**[1]

Received: 11 December 2021 / Accepted: 12 January 2022 / Published online: 8 February 2022

Abstract
Recent research in the field of electrochemical biosensors equipped with peptides and nanomaterials have been categorized, reviewed, and critically analyzed. Indeed, using these innovative biosensors can revolutionize biomedical diagnostics in the future. Saving lives, time, and money in this field will be considered as some main benefits of this type of diagnosis. Here, these biosensors have been categorized and evaluated in four main sections. In the first section, the focus is on investigating the types of electrochemical peptide-based nanobiosensors applied to detect pathogenic microorganisms, microbial toxins, and viruses. In the second section, due to the importance of rapid diagnosis and prognosis of various cancers, the electrochemical peptide-based nanobiosensors designed to detect cancer biomarkers have been reviewed and analyzed. In the third section, the electrochemical peptide-based nanobiosensors, which were applied to detect the essential and effective biomolecules in the various diseases, and health control, including enzymes, hormones, biomarkers, and other biomolecules, have been considered. Finally, using a comprehensive analysis, all the used elements in these biosensors have been presented as conceptual diagrams that can effectively guide researchers in future developments. The essential factors in evaluating and analyzing these electrochemical peptide-based nanobiosensors such as analyte, peptide sequence, functional groups interacted between the peptide sequences and other biosensing components, the applied nanomaterials, diagnostic techniques, detection range, and limit of detection have also been included. Other analyzable items such as the type of used redox marker and the location of the peptide sequence against the signal transducer were also considered.

Keywords Biosensor · Bioelectrochemistry · Peptide · Nanomaterials · Nanobiosensing · Electrochemical detection

Introduction

Reaching rapid, sensitive, selective, cheap, simple, portable, and repeatable detections is the primary goal of designing and developing optimized biosensors [1–4]. Optimal designing of biosensors can reply to critical diagnostic challenges in biomedical fields, especially diagnosing various diseases and environmental challenges (especially microbial pollutants and toxins) [5–8]. With the three components of biosensors (biorecognition element, signal transducer, and detector), if designed intelligently, the desirable results will be achieved, and biosensors can be considered as an alternative over current diagnostic laboratory methods [1, 3, 4, 9]. In recent years, enzymes [10–12], antibodies [13–15], aptamers [16–22], and peptides [23–29] have been used extensively as the biorecognition element in the structure of biosensors. Moreover, peptides in electrochemical biosensors can be directly employed as biorecognition elements or can play an indirect role by incorporating with the other biosensing elements, such as enzymes, aptamers, DNA, and antibodies. Overall, the purpose of applying the specific component(s) in the structure of biosensors is to provide more optimal biomedical diagnosing [30, 31]. Peptides are classified as momentous macromolecules that are derived from short polymerization of amino acids and have unique properties against proteins (proteins are produced by long polymerization of amino acids) and antibodies such as smaller size, simple preparation, diverse functionalization methods, and compatibility with different conditions [32–35]. In addition, peptide sequences can be designed

✉ Masoud Negahdary
mnegahdary@iq.usp.br

✉ Lúcio Angnes
luangnes@iq.usp.br

[1] Department of Fundamental Chemistry, Institute of Chemistry, University of São Paulo, Av. Prof. Lineu Prestes, 748, São Paulo 05508-000, Brazil

specially to have a high selectivity for diagnostic purposes. Due to the singular structures of various natural and synthetic amino acids, the design and providing peptides with the desired structures will be possible, while these peptides can reflect a biospecific role. Therefore, synthesizing new peptide sequences and identifying their function in different applications is fundamental [36, 37]. It should be noted that only nanobiosensors equipped with peptide sequences in their diagnostic components have been studied here, and it is obvious that the analytes of these biosensors may not be proteins only. Directed synthesis of peptides for applying in the design of biosensors and functionalizing them with functional molecules including thiol [23, 24], biotin [38, 39], amine [40], and carboxyl [41] leads to creating a suitable platform for stable and with a high-affinity immobilization of the biorecognition element on the surface of the signal transducers and also selective capturing the analyte molecules. When peptides are used as the biorecognition element, they can easily do self-assembling through several interactions, including intramolecular non-covalent bonds, hydrogen bonds, van der Waals, and π-π stacking [23–28]. Peptides can provide valuable quantitative detections based on the differences found in the electron transfer rate related to signal markers when these macromolecules captured/uncaptured the analyte molecules. The advantages of using peptides in the structure of biosensors include increasing the stability, sensitivity, selectivity, and reducing the design costs. In the design of the electrochemical biosensors, several (diagnostic) techniques, including cyclic voltammetry (CV), differential pulse voltammetry (DPV), electrochemical impedance spectroscopy (EIS), square wave voltammetry (SWV), linear sweep voltammetry (LSV), differential pulse anodic stripping voltammetry (DPASV), chronoamperometry (CA), electrochemical luminescence (ECL), and photoelectrochemical (PEC) techniques have been used [4, 42, 43]. One of the hot topics in recent decades in the field of biosensors is the use of nanomaterials to optimize the performance of these sensing platforms [16–20, 23, 24, 44–47]. In fact, the functional integration of nanomaterials with biomolecules has been a great benefit in the development of nanobiosensors. As it is clear, nanomaterials must be smaller than 100 nm in at least one dimension compared to bulk materials [48, 49]. Nanomaterials have different physicochemical properties compared to bulk materials due to increased surface area to volume ratio, and these advanced materials reflect a special reactivity. The application of nanomaterials in the structure of biosensing platforms has led to increased sensitivity (mostly as the signal amplifier), selectivity, stability, and a quick response against analytes [50–53]. The importance of detecting pathogenic microorganisms and their related toxins is very high, and many medical and health costs can be avoided by the accurate and rapid diagnosis of these analytes. Biomarkers have been introduced as a type of analyte for a large number of biosensors [54, 55]. In most cases, these protein biomolecules can represent a specific physiological or pathological condition that is applicable in the early-stage diagnosis or control of diseases and health monitoring [56, 57]. Determining the exact concentrations of biomarkers is applied to the early diagnosis and prognosis of many acute diseases such as cancers and myocardial infarction. So far, several review papers have been written in the field of peptide-based biosensors [34, 35, 58–64]. The purpose of this review was to present an updated revision in the field of electrochemical peptide-based nanobiosensors. So far, no review paper has been published in the field of peptide-based biosensors that exclusively emphasized nanomaterial-based biosensors. In addition, our focus was on reviewing the published researches in recent years only. We categorized the evaluated electrochemical peptide-based nanobiosensors by considering the type of analytes. The most important advantage of this review is the comprehensive analysis of the components contributed to these types of biosensors (including all reviewed papers) in the form of several unique diagrams, which can be considered certainly as an important map in the following researches. In summary, in this review, the assessment and performance analysis of the electrochemical biosensors equipped with peptides and nanomaterials have been followed; in the first section, the analyte of the evaluated biosensors were microorganisms (especially pathogenic bacteria), microbial toxins, and viruses. In the second section, the analytes were cancer biomarkers, and other biomolecules were reviewed in the third section. The last section presents a deep analysis of applied elements in the reviewed biosensors that can be considered for future research in this area.

Peptide-based nanobiosensors in microbiology (microorganisms, microbial toxins, and viruses)

Listeria monocytogenes and *Staphylococcus aureus* are two critical microbial species involved in the occurrence of food poisoning or gastrointestinal infections that can endanger general health [65]. A peptide-based biosensor abled to diagnose *Listeria monocytogenes* and *Staphylococcus aureus* as two major pathogen bacteria was reported [38]. The three-electrode system of this SWV based electrochemical biosensor included disposable electrical printed (DEP) microarray electrodes consisting of carbon, carbon, and Ag/AgCl as working, counter, and reference electrodes, respectively. In the first step of this biosensing platform setup, the working electrode's surface was modified with gold nanoparticles (Au NPs). The synthesizing solution consisted of 6 mM $HAuCL_4$ and 0.1 M KNO_3. Au NPs were produced on the surface of the working electrode by an electrodeposition method (20 times CV was recorded; scan rate: 50 mV s^{-1} and

the potential range was from − 200 to − 1200 mV). The characterization of the synthesized Au NPs was followed by scanning electron microscopy (SEM), and it was confirmed that the average size of synthesized particles was ~ 20–30 nm. Then, the working electrode was modified with 1-ethyl-3-(3-dimethylaminopropyl) carbodiimide/N-hydroxy-succinamide (EDC/NHS) solution and subsequently incubated with streptavidin solution. Afterward, two biotinylated peptide sequences were conjugated with the carboxylated magnetic nanoparticles (size of 50 nm) that immobilized on the surface of the working electrode through streptavidin covalent bond, and the whole of this assembly platform was applied as the biorecognition element; here, NH_2-Ahx-ETKVEENEAIQK Ahx-biotin peptide was considered for *Staphylococcus aureus*, and NH_2-Ahx-NMLSEVERE-Ahx-biotin peptide was considered for *Listeria monocytogenes*. The presence of EDC/NHS molecules on the surface of the electrode was led to the activation of the carboxyl group of magnetic nanoparticles for binding to the biotinylated peptide sequences. The presence of analytes (in this case: extracted bacteria proteases) has led to proteolytic cleavage of peptide sequences and releasing the magnetic nanoparticles from the surface of the working electrode. This phenomenon enhanced the electron transfer between the biorecognition element and transducer, whereas a quantitative biosensing platform was achieved with high affinity and selectivity. The presented signal-on biosensor could detect *Listeria monocytogene*s and *Staphylococcus aureus* in a range from 10 to 10^7 colony-forming units (CFU) mL^{-1} for both of them. In addition, the reported LOD for *Listeria monocytogenes* was about 9 CFU mL^{-1}, while this value was 3 CFU mL^{-1} for *Staphylococcus aureus*. In another research, a peptide-based biosensor was introduced to detect *Staphylococcus aureus* using a gold screen-printed electrode as the transducer and a peptide sequence as the biorecognition element [39]. This biosensor was developed for both electrochemical and colorimetric detection approaches. In order to find the electrochemical aims, a gold screen-printed electrode was applied as the signal transducer. The surface of this electrode was covered with streptavidin, and a peptide sequence (NH_2-Ahx-ETKVEENEAIQK Ahx-biotin) conjugated with magnetic nanoparticles (the applied magnetic nanobeads (average size diameter: 50 nm) were carboxylated, and initially, this functional group was activated by EDC/NHS; this nanostructure consisted of metallic nanoparticles covered by a layer of graphene-like carbon, size: 2 nm) that were covalently immobilized on the surface of the prepared electrode as the biorecognition element. The conjugated peptide with the magnetic beads was produced via activation of the carboxylated magnetic nanobeads by applying EDC/NHS against the N-terminal of the peptide followed by the incubation of the activated form with the peptide at room temperature. The applied peptide was biotinylated from the C terminal and could be bound with streptavidin on the surface of the transducer. The presence of Ahx linker in the peptide sequence was related to preventing steric hindrance and providing good access for protease to the cleavage the desired site. At this step, the prepared biosensor was ready to diagnose various concentrations of the analyte. Electrochemical measurements were followed using the SWV technique in the presence of ferro/ferricyanide ($[Fe(CN)_6]^{3-/4-}$) as the redox marker. In the presence of the analyte, the peptide cleaved, and magnetic nanoparticles released from the surface of the transducer. This event enhanced the electron transfer rate between the redox marker molecules and the transducer due to higher access of the redox marker molecules to the surface of the electrode. So, along with increasing the concentration of the analyte, the SWV peak currents were increased regularly. This described signal-on biosensor could determine *Staphylococcus aureus* in a linear range (10^2 to 10^8 CFU mL^{-1}) with a LOD of 3 CFU mL^{-1}. *Clostridium botulinum* can produce several types of botulism in humans by producing neurotoxins. These neurotoxins are the most toxic substances globally, so after considering ingestion and absorption in the intestine, these toxins sometimes cause muscle paralysis and human death [66]. In the research developed by Caratelli et al. (2021), a paper-based biosensor has been introduced to diagnose botulinum neurotoxins [67]. Here, botulinum neurotoxins A and C were evaluated while these toxins are derived from a Gram-positive bacterium (*Clostridium botulinum*). The working, counter, and reference electrodes in the mentioned biosensor were graphite, graphite, and Ag/AgCl, respectively. A peptide sequence (Cys-Ahx-Lys-Thr-Arg-Ile-Asp-Glu-Ala-Asn-Gln-Arg-Ala-Thr-Lys(Methylene blue (MB))-Met) was synthesized as the biorecognition element that was labeled with MB molecules (20 µM) as the redox marker from one side, and also this biorecognition element was modified with thiol group using cysteine residue from another side. Initially, the surface of the working electrode was modified with Au NPs, and then the peptide sequence was immobilized on the surface of it (Fig. 1, A). The Au NPs were synthesized by a mixture containing $HAuCl_4$ and sodium citrate at room temperature. The thiol group of the peptide was anchored to Au NPs through Au–S bound. At the next step, the electrochemical behavior of the biosensor was followed by the SWV technique (Fig. 1, B). Finally, the electrochemical behavior of the biosensor was evaluated in the presence of the analyte (botulinum neurotoxins A and C) (Fig. 1, C). As depicted in Fig. 1, in the presence of the botulinum neurotoxins, the applied peptides were cleaved. Neurotoxin A actuated on Gln-Arg, and the neurotoxin C involved the Arg-Ala bond. The cleavage event was led to

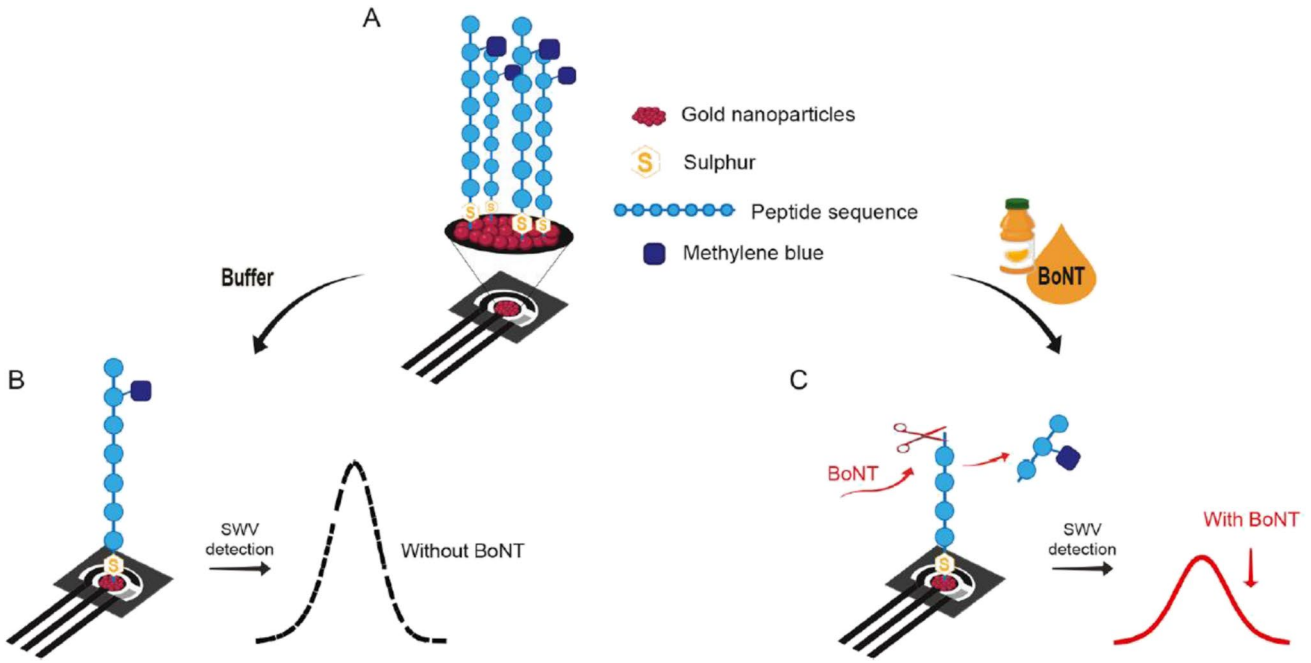

Fig. 1 A peptide-based biosensor for detecting botulinum neurotoxins **A** and **C**; permission number: 5091590989983

reducing redox marker molecules that found a significant decrement in SWV peak current (Fig. 1, C). This signal-off biosensor detected these neurotoxins in a linear range from 0.01 to 10 nM. The reported LOD for both analytes was 10 pM.

Candida species are well-known yeast fungi that have been considered in many kinds of research in medicine, the health of the food industry, and biology. Numerous species of this yeast cause candidiasis of the skin, oral candidiasis, candidal vaginitis, candidal onychomycosis (nail infection), and other superficial infections. Sometimes, the host's immune system is weakened or defective for some reason, and candidates can develop dangerous systemic infections in the blood or internal organs [68]. A peptide-based biosensor has been reported for diagnosis of *Candida* yeasts (*C. krusei*, *C. glabrata*, *C. albicans*, and *C. tropicalis*) using a gold electrode (GE), a thin film of poly (3-thiophene acetic acid), titanium dioxide nanoparticles (TiO_2 NPs, size ~ 9 nm), and an antimicrobial peptide (Clavanin A, sequence: VFQFLGKIIHHVGNFVHGFSHVF [69]) as the biorecognition element [70]. The TiO_2 NPs were amine-functionalized, and in order to synthesize, the TiO_2 NPs were added to a flask containing dimethyl sulfoxide (DMSO), and then after 60-min ultrasonication, the desired amount of (3-aminopropyl) triethoxysilane (APTES) was added to the mixture. Finally, the product was stirred, washed (with methanol), filtered, and dried (temperature: 60 °C). In the initial step of the biosensing setup, the surface of the GE as the working was modified with 3-thiophene acetic acid by CV electropolymerization. Afterward, the achieved polymer could capture TiO_2 NPs. The captured nanoparticles enhanced the active area for the working electrode against bioelectrochemical interactions. It should be considered that the connection between the polymer and TiO_2 NPs was based on the carboxyl groups (activated by EDC (0.4 M): NHS (0.1 M)) of polymer and amine functional group of TiO_2 NPs. The atomic force microscopy (AFM) study confirmed that the presence of the mentioned nanoparticles was led to an increase in the active surface area of the polymer from 64 to 73 nm. Finally, Clavanin A was immobilized on the surface of the GE through a covalent bond and applied for capturing analyte molecules. Here, the counter and reference electrodes were platinum and Ag/AgCl, respectively. The biosensing performance was evaluated using the charge transfer resistance (Rct) followed by EIS, and the Rct was increased along with the increment concentrations of analytes. The highest Rct (2.95 kΩ) was found at the highest concentration of *C. albicans* (10^6 CFU mL^{-1}). The mentioned biosensor detected *Candida* yeasts in a range between 10^1 and 10^6 CFU mL^{-1}, and the reported LOD was about 2–3 CFU mL^{-1}. *E. coli* is a rod-shaped gram-negative bacterium. Most strains of *E. coli* are harmless, but some species can cause severe food poisoning in humans. *E. coli* O157:H7, also known as enterohemorrhagic *E. coli* (EHEC), was identified as a cause for severe and even fatal complications such as hemolytic uremic syndrome, leading to kidney failure [71]. In a research, a peptide-based biosensor was designed to diagnose pathogen *E. coli* O157:H7 using a translocated intimin receptor peptide

and a modified carbon screen-printed electrode with Au NPs [72]. First, the surface of the working electrode was modified with Au NPs as the signal amplifier. The Au NPs were electrodeposited on the surface of the working electrode through an electrodeposition process directed by a synthesis solution containing 1 mM of $HAuCl_4$ and 0.5 M of H_2SO_4. The surface morphology and the size of synthesized nanoparticles were characterized via SEM, and the average diameter size of particles was about 90 nm. Subsequently, a peptide sequence (QKVNIDELGNAIPSGVLKDD) as the biorecognition element was immobilized on the surface of the mentioned modified electrode. It should be considered that the peptide sequence contained a cysteine residue in the N-terminal region. The immobilization process was performed via an Au–S bond between cysteine residue of the peptide and Au NPs. Then, the prepared biosensor was applied to detect various concentrations of *E. coli* O157:H7 via EIS technique while $[Fe(CN)_6]^{3-/4-}$ was applied as the redox marker. Each analyte concentration showed a direct association toward reducing the electron transfer rate between the molecules of the redox marker and the surface of the transducer. The highest reduction in the electron transfer rate was found for the applied maximum concentration of the analyte. It seems the captured molecules of the analyte by the biorecognition element with a high affinity increased the distance between the molecules of the redox marker and the surface of the signal transducer. The presented biosensor could detect the analyte in a range up to 500 CFU mL^{-1} with a LOD ~ 2 CFU mL^{-1}. Norovirus is considered a type of virus that causes inflammation of the stomach, intestines, or both (acute gastroenteritis). Diarrhea, vomiting, stomach pain, fever, headache, and body aches are some of the symptoms of norovirus [73]. In a study, a peptide-based biosensor was introduced to diagnose norovirus in the oyster sample using Au NPs–decorated tungsten disulfide nanoflowers (WS_2 NF/Au NPs) [74]. In order to produce nanomaterials, WS_2NF was produced via a hydrothermal method using tungsten (VI) chloride (WCl_6) and thioacetamide (TA) as a reducing and sulfurizing reagent. Here, TA was broken in the presence of H_2O at a high temperature and was led to produce H_2S gas. At the next step, this achieved gas was reacted with WCl_6 to produce WS_2NF (Fig. 2). The analysis synthesizing of WS_2NF by x-ray diffraction (XRD) confirmed that this nanostructure was presented as 2D nanosheets and the temperature changes showed a direct effect on the product features. The SEM characterization was also followed for various synthesizing conditions of WS_2NF, and the results confirmed the largest surface area was found when the synthesis temperature was 280 °C. The produced flower-like shapes at this condition showed an average size of about 4–5 µm. Afterward, the obtained WS_2NF nanostructure was functionalized with 3-mercaptopropionic acid (MPA) using n-butyllithium/hexane solution to equip the surface of WS_2NF nanostructure with the carboxyl group that was led to the growing of Au NPs on it. In fact, the decoration of Au NPs on WS_2NF nanostructure followed by adding $HAuCl_4$

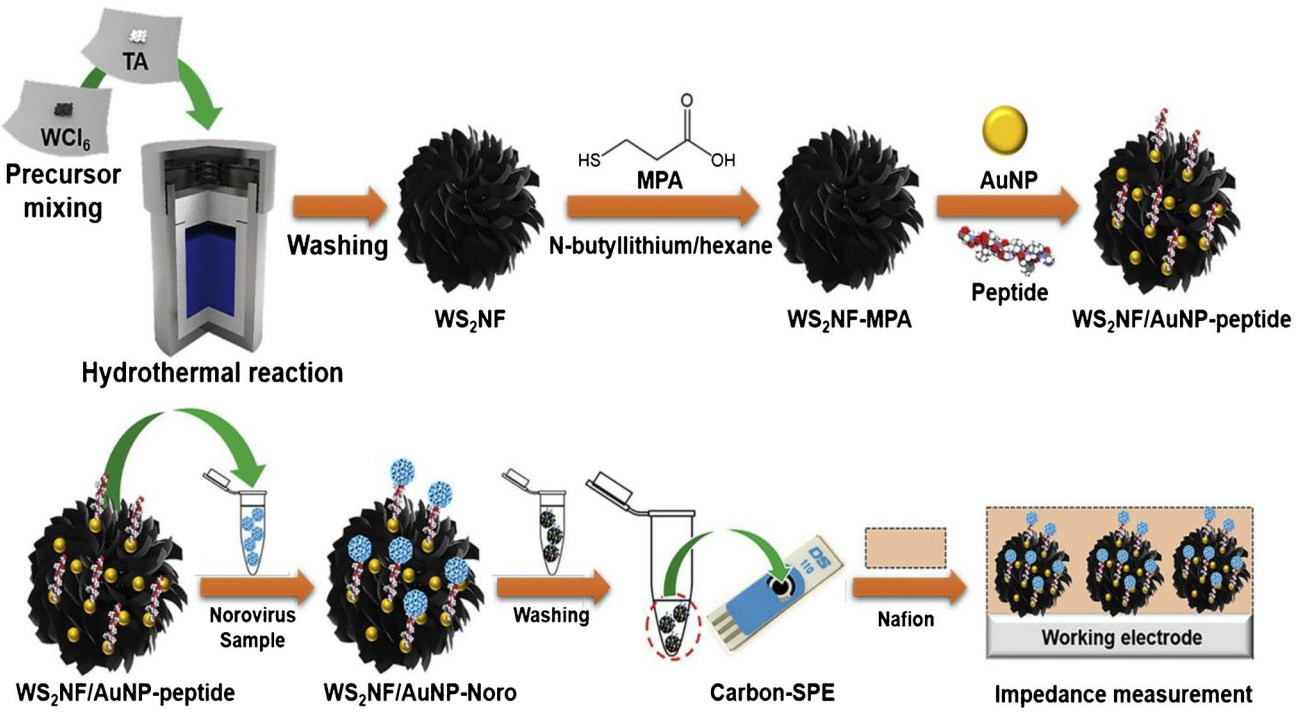

Fig. 2 A peptide-based biosensor designed to detect norovirus in the oyster sample; permission number: 5223220570549

and 0.3 M $NaBH_4$ into a solution containing WS_2NF-MPA. The morphology of WS_2NF had a direct effect on the carrying capacity against Au NPs. So the optimized production of WS_2NF enhanced the immobilization rate of the peptide molecules as the biorecognition element on the surface of the working electrode. At the next step, the peptide sequence (QHKMHKPHKNTKEKEKEKEGGGGSGGGGSC) as the biorecognition element and with a desirable affinity against the analyte was immobilized on the mentioned nanocomposite (WS_2NF/Au NPs) through cysteine residue on the C-terminal part (Fig. 2). The finally obtained mixture (WS_2NF/Au NPs-peptide) was then used to modify the surface of the carbon screen-printed electrode and apply as a biosensing platform to the diagnosis of norovirus using the EIS technique. In the presence of norovirus, the peptide strands could capture the molecules of norovirus, and the electron transfer rate created by redox marker ($[Fe(CN)_6]^{3-/4-}$) between the electrolyte and transducer was reduced along with the concentration of the analyte. This event was led to enhancing the impedance on the surface of the signal transducer. This biosensor reported diagnosis against norovirus concentrations in a linear range from 0 to 10^4 copies mL^{-1} while the reported LOD was equal to 6.21 copies mL^{-1}.

In Table 1, the main features of the electrochemical biosensors equipped with peptides and nanomaterials have been cited; the analytes for these biosensors were microorganisms, microbial toxins, and viruses.

Peptide-based nanobiosensors in the diagnosis of cancers

Matrix metalloproteinases (MMPs) are a group of zinc- and calcium-dependent endopeptidases that are responsible for the rheolytic ability of many extracellular matrix compounds (collagens, proteoglycans, and glycoproteins); these enzymes are led to intensifying the process of inflammatory responses [80]. MMPs also have an essential role in cell functional activities, including differentiation, proliferation, apoptosis, migration, and angiogenesis. There are several types of MMPs, whereas, between all, the MMP-2 and MMP-7 are involved in metastasis and prognosis of cancers [81]. A peptide-based biosensor was developed to determine MMP-2 using the silver nanoparticles (Ag NPs) and two peptide sequences immobilized on the surface of a GE as the signal transducer [82]. First, the surface of the working electrode was modified with peptide 1 (FGPLGVRGKGGC), and this peptide established interactions with N-terminal phenylalanine (F) residue, cucurbit[8]uril (CB[8], a macrocyclic receptor (capable of connecting two aromatic amino acid residues based on host–guest recognition mechanism), and a C-terminal of 11-mercaptoundecanoic acid. At the next step, peptide 2 (FGGGASLWWSEKL) was conjugated with Ag NPs and then immobilized on the surface of the working electrode and could be connected to peptide 1 through CB [8] molecules. The peptide conjugated with Ag NPs was synthesized from a mixture solution containing 100 ng μL^{-1} peptide 2 and 0.2 mM $AgNO_3$. The mixture was stirred and then was reduced by adding 2 mM $NaBH_4$. Finally, reaching the yellow color confirmed having the peptide conjugated with Ag NPs. The peptide conjugated with Ag NPs was characterized by transmission electron microscopy (TEM), X-ray photoelectron spectroscopy (XPS), and UV–vis spectrophotometry. The results of the TEM study showed that the average diameter size of Ag NPs was 10 nm, while the XPS study confirmed indirect electroreduction of Ag 3d5/2 (binding energy: 367.5 eV) and Ag 3d3/2 (binding energy: 373.5 eV). In addition, the UV–vis study showed the absorption peak for Ag NPs at the 405-nm region. The mechanism of biosensing was based on host–guest recognition, and in the absence of analyte, the enhanced conductive area obtained by Ag NPs could produce a high electron transfer rate, and the peak current of DPV was in the maximum value (redox marker: $Fe(CN)_6]^{3-/4-}$). In the presence of MMP-2 molecules, the proteolytic cleavage occurred in peptide 1 (between amino acids G and V), and this cleaved peptide has led to releasing peptide 2-Ag NPs from the surface of the electrode. This event was an apparent reason for the considerable reduction in the electron transfer rate (reducing peak current). The described signal-off biosensor could detect the mentioned enzyme in a range from 0.5 pg mL^{-1} to 50 ng mL^{-1}, and the reported LOD was 0.12 pg mL^{-1}. In another research, a peptide-based biosensor was designed to detect MMP-2 using a GCE as the signal transducer and the Au@Pt bimetallic nanorods as catalyst (nanozyme) [83]. First, the surface of the signal transducer was modified with chitosan (CS) and graphene quantum dots (GQDs)-COOH nanocomposites. Afterward, the EDC/NHS solutions were added on the surface of the signal transducer to activate the carboxyl group, and then a peptide sequence (KGRVGLPGC) was immobilized on it through an amide reaction. This peptide was applied as the biorecognition element. Unwanted active sites of the biorecognition element were blocked with bovine serum albumin (BSA). Subsequently, Au@Pt nanorods were added to the surface of the transducer and could be bound to the cysteine group of the peptide sequence through Au–S interactions. In order to synthesis of the Au@Pt nanorods, initially, the Au nanorods were chemically produced through a reduction-based procedure. The synthesizing solution included a mixture of 0.1 M cetyltrimethyl ammonium bromide (CTAB), 24 mM $HAuCl_4$, and 0.01 M $NaBH_4$. In another separate procedure, Au nanorods were synthesized by a seed-mediated growth method in a mixture solution containing 0.5 M H_2SO_4, 10 mM $AgNO_3$, 0.1 M ascorbic acid (AA), 24 mM $HAuCl_4$, 0.1 M CTAB, and 150-µL seed solution. Afterward, Au@Pt

Table 1 Main features of electrochemical biosensors equipped with peptides and nanomaterials designed for diagnosing microorganisms, microbial toxins, and viruses

Analyte	Signal transducer	Peptide	Functional group interacted with the peptide sequence	Nanomaterial (s)	Detection technique	Detection range	LOD	Ref
Botulinum neurotoxin serotype A and C	Paper-based electrode	CLYRIDEANQRATLM	Thiol	Au NPs	SWV	Up to 1 nM	10 pM	[67]
Botulinum neurotoxin A	GE	SNAP-25-GFP	Carboxyl	rGO	DPV	1 pg mL^{-1}–1 ng mL^{-1}	1 pg mL^{-1}	[75]
Mycotoxin deoxynivalenol (DON)	GE	Mimotope peptide	–-*	Au NPs	SWV	0.1–10,000 pg mL^{-1}	0.07 pg mL^{-1}	[76]
Zearalenone (ZEN)	Glassy carbon electrode (GCE)	DAVILLM	Carboxyl	Carbon nanohorns (CNHs)/ Au nanocones (Au NCs)	EIS	10^{-6}–1 ng mL^{-1}	1×10^{-6} ng mL^{-1}	[77]
Listeria monocytogenes/ Staphylococcus aureus	DEP microarray electrode	ETKVEENEAIQK	Biotin/ amino hexanoic acid (Ahx)	Carboxylated magnetic nanoparticles	SWV	10–10^7 CFU mL^{-1}	Listeria monocytogenes: 9 CFU mL^{-1}; Staphylococcus aureus: 3 CFU mL^{-1}	[38]
Staphylococcus aureus	Gold screen-printed electrode	ETKVEENEAIQK	Biotin/ amino hexanoic acid (Ahx)	Carboxylated magnetic nanobeads	SWV	10^2–10^8 CFU mL^{-1}	3 CFU mL^{-1}	[39]
Promastigote surface antigen (PSA) PSA Leishmania	GE	CTSSAPVARAAGT GDFTEEQRTNTL	NH_2/ Carboxyl	Chitosan Nanofibers	EIS	2.5–10 pg mL^{-1}	0.2 pg mL^{-1}	[78]
Candida yeasts (C. krusei, C. glabrata, C. albicans, and C. tropicalis)	GE	Clavanin A: VFQFLGKIIHHVGNFVHGFSHVF	Non-polar amino acid residues (FLPII)	TiO_2 NPs	EIS	10^1–10^6 CFU mL^{-1}	2–3 CFU mL^{-1}	[70]
S. aureus, E. faecalis, P aeruginosa, S. typhimurium and E. coli	GE	Clavanin A: VFQFLGKIIHHVGNFVHGFSHVF	Thiol	Au NPs	EIS	10^1–10^4 CFU mL^{-1}	10 CFU mL^{-1}	[79]
Norovirus	Carbon screen-printed electrode	QHKMHKPHKNTKEKEKEKEGGGGSGGGGSC/ QHKMHKPHKNTKEKEKEKEGGGGSGGGGSMHGKTQATSGTIQS	Thiol	WS_2 NF/Au NPs	EIS	Up to 10^4 copies mL^{-1}	6.21 copies mL^{-1}	[74]
E. coli O157:H7	Carbon screen-printed electrode	QKVNIDELGNAIPSGVLKDD	Thiol	Au NPs	EIS	Up to 500 CFU mL^{-1}	2 CFU mL^{-1}	[72]

* The functional group interacted with the peptide sequence not reported or not applicable.

nanorods were produced from a mixture solution containing Au nanorods, 2 mM H_2PtCl_4, and 0.1 M AA. The characterization of the synthesized Au@Pt nanorods was followed by the microscopic analysis (TEM, SEM) and EDS. The analysis showed that the Au@Pt nanorods produced from the seed-mediated growth method had an average length and width equal to 43.3 ± 4.9 nm and 11.2 ± 2.3 nm, respectively. The found size for the chemical reduction–based method was with an average length and width equal to 57.9 ± 4.9 nm and 14.5 ± 2.6 nm, respectively. Au@Pt nanorods as the signal amplifier showed a role as an oxidase in the catalytic reaction of 3,3′,5,5′-tetramethylbenzidine (TMB) as the redox marker and also for the dissolved O_2 in a hydrogen peroxide (H_2O_2)-free system (TMB-O_2 system). The electrochemical measurements were performed via DPV technique in the presence of various concentrations of MMP-2, and the peak current of DPVs was reduced along with the enhancing concentrations of MMP-2. The reported detection range for the presented signal-off biosensor was from 0.5 to 100 ng mL^{-1} with a calculated LOD of about 0.18 ng mL^{-1}. Prostate-specific antigen (PSA) is a glycoprotein found only in the epithelium of the prostate gland. PSA is a leading and valuable tumor marker the diagnosis and prognosis of prostate cancer [45]. In the research done by Ye et al. (2020), a peptide-conjugated hemin/G-quadruplex (DNAzyme-peptide) was applied as the biorecognition element of a PSA biosensor [84]. A three-electrode system was applied for the electrochemical measurements while the working, counter, and reference electrodes were GCE, platinum, and Ag/AgCl, respectively. All the CV electrochemical evaluations were followed in a solution containing $[Fe(CN)_6]^{3-/4-}$ as the redox marker, while DPVs were recorded in phosphate-buffered saline (PBS) (pH 7.4) containing 2.5 mM H_2O_2. The surface of the working electrode was modified first with molybdenum diselenide@reduced graphene oxide ($MoSe_2$@rGO) nanocomposite through the chemical absorption at room temperature and then with Au NPs through electrochemical deposition (synthesis solution: $HAuCl_4$, potential: − 200 mV, time: 15 S) (Fig. 3, B). In order to synthesize the $MoSe_2$@rGO nanocomposite, a mixture solution containing 5 mg mL^{-1} GO, ethanol, and oleic acid was prepared, and then $(NH_4)_2MoO_4$ and Se powder was added. Then, after performing stirring, the mixture was kept for 72 h at 200 °C and then cooled naturally. At the next step, after centrifuging

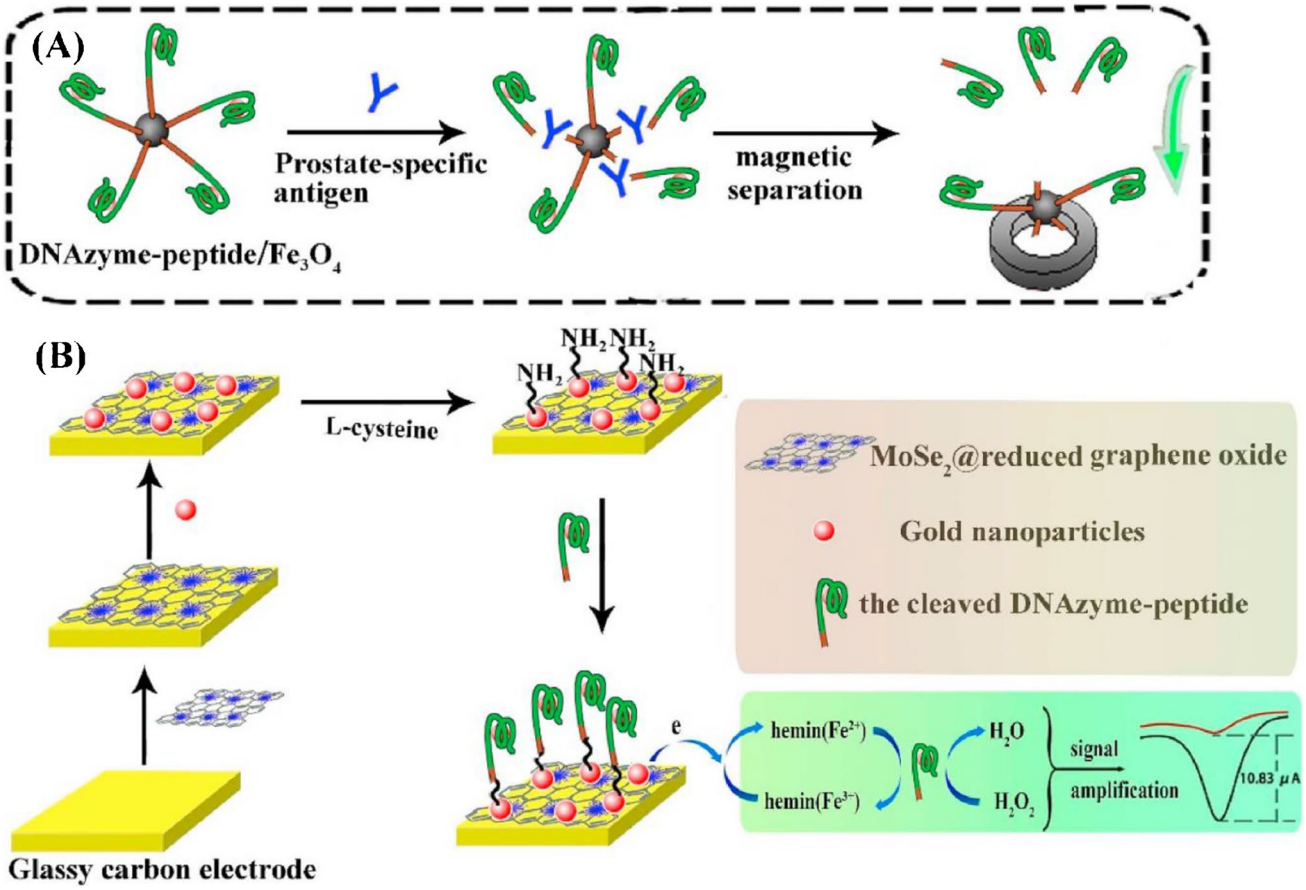

Fig. 3 A peptide-based biosensor (a modified GCE with $MoSe_2$@rGO nanocomposite, Au NPs, and DNAzyme-peptide) for the detection of PSA; permission number: 5096810262140

and washing, the mixture was kept at 200 °C overnight and then was annealed 2 h at 300 °C. Finally, the desired amount of the obtained nanocomposite was suspended in ethanol before use. Afterward, the modified electrode with $MoSe_2$@rGO/Au NPs was immersed in an L-cysteine solution, and the Au–S bond was established between the thiol molecules of cysteine and Au NPs, and the unwanted interactions were blocked by hexanethiol. Next, the magnetic DNAzyme-peptide-Fe_3O_4 probe was prepared via labeling of peptide (HSSKLQ)-conjugated hemin/G-quadruplex (DNAzyme-peptide) hybrid with the mesoporous Fe_3O_4 (70 nm)-COOH and then incubated with several PSA concentrations at 37 °C. Subsequently, the PSA molecules as the analyte were led to cleavage of the probe, and the magnetic separation process occurred where Fe_3O_4 molecules were removed from the probe (Fig. 3, A). In another stage, the amine group of cysteine could covalently interact with the carboxyl group of the released DNAzyme-peptide. It should be noted that the activation of the carboxyl group was performed by EDC/NHS (2:1). Finally, the hemin molecules of the DNAzyme-peptide have produced a detectable electrochemical signal that is also amplified in the presence of $MoSe_2$@rGO/Au NPs nanomaterials. In order to evaluate the electrocatalytic activity of the biorecognition element, H_2O_2 was added to a PBS solution up to 2.5 mM, and the peak current of DPV increased regularly. In the presented research, the applied peptide sequence showed two separate applications, including the biorecognition element against the analyte and incrementing the enzyme activity of hemin/G4 (that improved the sensitivity). This signal-on biosensor detected the various concentrations of PSA in a linear range from 1 fg mL^{-1} to 80 ng mL^{-1} while the reported LOD was equal to 0.3 fg mL^{-1}.

In another research, a peptide/antibody-based biosensor was designed for diagnosing the PSA using the modified GCE with polydopamine-coated boron-doped carbon nitride (Au@PDA@BCN) nanocomposite and also with a peptide bioconjugated with AuPt metallic nanoparticles and manganese dioxide (MnO_2)–functionalized covalent organic frameworks (AuPt@MnO_2@COF) nanocomposite in a sandwich assay platform [85]. First, COF was synthesized from a mixture containing mesitylene:dioxane (1:1), 1,2,4,5-Tetrakis-(4-formylphenyl) benzene (TFPB), and 1,4-diaminobenzene (PPDA). In this solvothermal method, the prepared mixture was sonicated, and after adding the desired amount of 6 M acetic acid, it was kept at 120 °C for 72 h. Then, the mixture cooled naturally and subsequently washed with tetrahydrofuran and acetone to attain the COF solid. In another procedure, a solution consisting of COF and $HClO_4$ was prepared and then sonicated. At the next step, $KMnO_4$ was added to the prepared mixture and stirred and sonicated, respectively. Finally, the centrifugation was performed, and the mixture was washed with the deionized water that at this step, the MnO_2@COF composite was obtained. Another procedure was applied to synthesis AuPt@MnO_2@COF nanocomposite. Here, a mixture containing MnO_2@COF and ethanol was prepared. At the next step, $HAuCl_4$ and H_2PtCl_6 were added to the mixture, respectively. Then, the $NaBH_4$ was added to the mixture as a reductant. Finally, after centrifugation and washing, the AuPt@MnO_2@COF nanocomposite was achieved. In order to design the biosensing platform, the GCE surface was modified with Au@PDA@BCN nanocomposite, and then the PSA antibody (Ab1) was immobilized on the surface of the GCE, and at the next step, the unwanted active sites were blocked with BSA. Afterward, the analyte was added to the surface of the mentioned signal transducer. The Ab1 could capture the analyte molecules. On the other side, the MnO_2@COF composite was prepared, and then $HAuCl_4$ and H_2PtCl_6 were mixed with it to obtain AuPt@MnO_2@COF nanocomposite. Subsequently, MB as the redox marker and a peptide sequence (CGGGGMERCPIK-MFYNLGSPYMNI) as a part of the biorecognition element was added to obtain MB/AuPt@MnO_2@COF and peptide/MB/AuPt@MnO_2@COF, respectively. Finally, the peptide/MB/AuPt@MnO_2@COF was added to the surface of the signal transducer, and the PSA sandwich assay platform was completed. The assays of PSA were performed via DPV technique in a three-electrode system where the redox marker was MB. The principle detection of PSA was based on these strategies. After modifying the GCE with Au@PDA@BCN, the conductivity of the signal transducer was enhanced based on the applied nanocomposite. At the next step, after immobilization of Ab1, the conductivity of the signal transducer was reduced, and this phenomenon confirmed the successful immobilization of Ab1. When the BSA was applied, the signal transducer conductivity was further decreased. It should be noted that the minimum conductivity of the signal transducer for electron transfer was found when the PSA molecules (analyte) were added to the surface of the signal transducer. However, when the Pep/MB/AuPt@MnO_2@COF nanocomposite was added on the transducer surface as the final step, the conductivity was enhanced due to the presence of AuPt NPs and MnO_2@COF core–shell structure. The presented signal-on biosensor could detect PSA in a linear range from 0.00005 to 10 ng mL^{-1} with a LOD of about 16.7 fg mL^{-1}. In another research, a PEC peptide-based biosensor was developed for early detection of PSA by applying cadmium telluride (CdTe)/TiO_2 electrode and copper sulfide (CuS) nanocrystals [40]. Here, a composite (CdTe/TiO_2) with a good photocurrent response signal was produced as the signal transducer. In order to produce this signal transducer, TiO_2 nanotubes (60 nm) as the base of this signal transducer were synthesized through anodization of a titanium sheet. Afterward, a CdTe QDs film (4 nm) was synthesized and then immobilized on the surface of the considered electrode (CdTe-TiO_2). At the next step,

an amine-functionalized peptide sequence (CEHSSKLQLAK-NH_2) as the biorecognition element was immobilized on the surface of the prepared electrode. It should be considered that the peptide solution contained peptide, EDC, and NHS. The 6-mercapto-1-hexanol (MCH) was used to block the unwanted peptide binding sites on the surface of the signal transducer. Subsequently, DNA R1 (5′-COOH-TATTAACTTTACTCC-3′) and DNA R2 (5′-TCAGCGGGGAGGAAGGGAGTAAAGTTAATA-3′) were immobilized on the surface of the signal transducer, respectively. Next, the hairpin probe H1 (5′-CTTCCTCCCCGC TGACAAAGTTCAGCGGGG-3′) and the hairpin probe H2 (5′-TCA GCG GGGAGGAAGCCCCGCTGAACTTTG-3′) were added on the surface of the signal transducer that created dsDNA in interaction with DNA R1 and DNA R2. Finally, the conjugated CuS nanocrystals (size: 5 nm) with doxorubicin (Dox) solution were immobilized on the dsDNA, and the prepared biosensor was applied to detect various concentrations of PSA. All PEC measurements were followed using a three-electrode system in PBS (0.1 M, pH 7.4) where the mentioned TiO_2 nanotubes electrode was applied as the working, and the counter and reference electrodes were platinum and Ag/AgCl, respectively. In the presence of PSA, due to a high affinity between the peptide and analyte, the peptide was cleaved, and DNA/Dox-CuS probes were released from the surface of the transducer, and the photocurrent intensity was enhanced along with the increment the concentration of the analyte. This signal-on biosensor offered a quantitative detection method for PSA diagnosis in a linear range from 0.005 to 20 ng mL^{-1}, and the LOD was 0.0015 ng mL^{-1}. Alpha-fetoprotein (AFP) is a protein commonly produced by the growing baby's liver and yolk sac during pregnancy. The levels of AFP decrease after birth. High levels of AFP in the blood of non-pregnant women and men can be a sign of serious cancers, especially for the liver, testicles, and ovaries [86]. In a research, a biosensor has been designed for early diagnosing of AFP using a modified GCE with conducting polymer polyaniline (PANI) and partial D-amino acids (pD-peptide) [87]. The electrochemical assays were followed in a PBS solution containing $[Fe(CN)_6]^{3-/4-}$ as the redox marker. The applied three-electrode system has consisted of GCE, platinum, and Ag/AgCl electrodes as working, counter, and reference, respectively. The DPV was the main technique for determining the various concentrations of AFP. Initially, the surface of the working electrode was modified with a thin layer of PANI film (60–130-nm nanoparticles) through an electrodeposition procedure (constant current: 0.01 mA cm^{-2} for 60 min). Then, 3-sulfo-N-hydroxysuccinimide ester sodium salt (sulfo-SMCC) was immobilized on the surface of the modified electrode with PANI film. Afterward, the AFP aptamer (5′-GGCAGGAAGACAAACAAGCTTGGCGGC GGGAAGGTGTTTAAATTCCCGGGTCTGCGTGGTCTG TGGTGCTGT-SH-3′) was added on the surface of the electrode. Subsequently, pD-peptide (CPPPPEKEKEKEK) was also added to the surface of the working electrode (Fig. 4). The presence of unnatural D-amino acids in the peptide sequence prevented enzymatic degradation and incremented the antifouling capability. The reason for using sulfo-SMCC was the application of it as a cross-linking agent (via covalent bond) between the amine groups of the PANI and the thiol group of aptamer and cysteine residue of the peptide. The fabricated biosensor was used against various concentrations of AFP. In the presence of AFP molecules, the conductivity of the signal transducer was reduced, and the lowest electron transfer rate (maximum decrement in the peak current of DPV) was achieved when the maximum concentration of AFP was applied. The mentioned signal-off biosensor detected AFP linearly in a range from 0.1 fg mL^{-1} to 1.0 ng mL^{-1}, and the LOD was 0.03 fg mL^{-1}.

MicroRNAs (miRNAs), as a large subset of non-coding RNA (18–25 nucleotides), are evolutionarily conserved. These biomolecules control gene expression after transcription by inhibiting mRNA translation and also inducing the mRNA degradation by binding to the untranslated region at the end of mRNAs [88]. The interaction of miRNAs with target genes determines their role in growth, programmed death of cells, cell differentiation, and proliferation, whereas

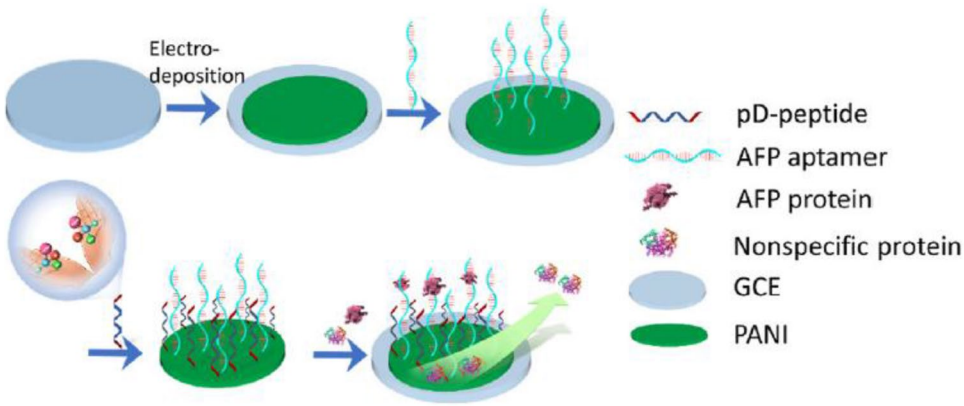

Fig. 4 A peptide-based biosensor for the detection of AFP; the GCE as the transducer was modified with PANI, a peptide, and also an aptamer; permission number: 5105670878712

it confirms the direct role of miRNAs in cancer. The structure of microRNAs indicates that many miRNAs are abnormally expressed in cancer specimens. In addition, functional differences between different types of tumors and different stages of cancerous cells are associated with the expression of miRNAs. In a study, miRNA-192 has been detected by a biosensor designed using a nanocomposite containing GO decorated peptide nanotubes [89]. Initially, to produce the nanocomposite, the FF sequence as the contributing peptide was added to 1,1,1,3,3,3-Hexafluoro-2-propanol and deionized water; then, the self-assembled peptide nanotubes (PNT) were achieved. PNT has many advantages, including simple production, high stability, and high biocompatibility [90]. Then, the same concentration (1:1) of GO and PNT were mixed, and the considered nanocomposite (PNT-GO) was achieved. It is assumed that the interactions between the PNT and GO are hydrogen bonding and π-π stacking. Electrochemical measurements of analyte were performed via EIS technique in a solution containing $[Fe(CN)_6]^{3-/4-}$ as the redox marker, and this electrolyte was in touch with a three-electrode system including a pencil graphite electrode (PGE) as the working, a platinum wire as the counter and an Ag/AgCl as the reference. The surface of the PGE was modified with PNT-GO, and then the miRNA-192 oligonucleotide (5′-GGCTGTCAATTCATA GGTCAG-Amino-3′) was immobilized as the biorecognition element on the enhanced and optimized surface of the modified electrode. During biosensing, the electron transfer resistance (Ret) was increased along with the increment of analyte concentrations due to the accumulation of the bound analyte with the biorecognition element molecules and also the reduced redox marker molecules on the surface of the signal transducer. The presented biosensor could detect miRNA-192 in a linear range from 10 fM to 1 nM, and the found LOD was 8 fM. In another research, Au NPs assembled peptide nanotubes (Au NPs-PNT) were applied in a biosensor to diagnosis miRNA 410 (5′-AGGUUGUCUGUG AUGAGUUCG-3′) as a tumor marker related to prostate cancer [91]. Here, the applied peptide was FF. In order to synthesize Au NPs-PNT nanocomposite, the FF was mixed with 1,1,1,3,3,3-Hexafluoro-2-propanol and subsequently with $HAuCl_4$ while heated at 60 °C. It should be noted that Au NPs (size: 20–40 nm) were attached to the PNT through physical absorption. At the next step, the PGE was applied as the working electrode and immersed in the solution containing Au NPs-PNT, and then the modified electrode was achieved (PGE-Au NPs-PNT). Finally, the DNA probe (5′-CGAACTCATCACAGACAACCT-SH-3′) was immobilized on the surface of PGE-Au NPs-PNT, and the biosensor was ready to quantify the different concentrations of miRNA 410. The Au–S covalent bond was established between the thiol group of DNA probe and Au NPs. All electrochemical measurements were followed in a solution containing $[Fe(CN)_6]^{3-/4-}$ as the redox marker, and the reference and counter electrodes were saturated calomel and platinum, respectively. The proposed detection mechanism was similar to other reported research by other authors [89]. The mentioned impedimetric biosensor could detect miRNA 410 in a linear range from 10 fM to 300 pM, while the reported LOD was about 3.90 fM. In Table 2, the main features of the electrochemical biosensors equipped with peptides and nanomaterials with remarkable selectivity and sensitivity to quantify cancer biomarkers have been cited.

Peptide-based nanobiosensors in the diagnosis of other important biomolecules

Exosomes are small (30–200 nm) vesicles found primarily in blood, urine, saliva, sperm, and serum [118]. Exosomes play an essential role in various critical biological processes such as the immune and inflammatory response, pregnancy, blood coagulation, and angiogenesis. These molecules are also involved in pathological processes, including neurological disorders, cancer, infectious, and cardiovascular diseases. The development of biosensors for the detection of tumor exosomes in blood for cancer diagnostics is highly desirable. In this direction, a peptide-based ECL biosensor has been introduced for diagnosing phosphatidylserine-positive tumor exosomes [117]. This analyte is considered the primary biomarker of ovarian cancer. Here, electrochemical measurements were performed using a three-electrode system while the working, counter, and reference electrodes were GCE, platinum, and Ag/AgCl, respectively. The surface of the working electrode was modified with a thin layer of Au nanostructure through an electrodeposition process of $HAuCl_4$ solution at a negative potential (−0.2 V for 30 s). Afterward, a peptide sequence (FNFRLKAGAKIRFGRGC), which actuates as the biorecognition element, was immobilized on the surface of the modified electrode. Unwanted active sites of the peptide strands on the surface of this electrode were blocked with BSA solution. Then, the established self-assembled monolayer of the peptide was applied for the detection of various various concentrations of the analyte. On the other side, peptide Luminol (Lum)-Au NPs@Graphitic carbon nitride (g-C_3N_4 nanosheets, characterized by TEM: average hydration size: 93 nm) core–shell nanoprobe was prepared and modified the surface of the working electrode, and this prepared sandwich structure was used for ECL measurements. Here, g-C_3N_4 nanosheets were synthesized from heating (550 °C for 240 min) melamine. The product was then cooled at room temperature naturally and in order to the dispersibility, the produced nanostructure was added to 5 M HNO_3. In another experiment, Lum-AuNPs were synthesized from a mixture containing 0.1 M NaOH

Table 2 Main features of electrochemical biosensors equipped with peptides and nanomaterials designed for diagnosing cancer biomarkers

Analyte	Signal transducer	Peptide	Functional group interacted with peptide sequence	Nanomaterial (s)	Detection technique (s)	Detection range	LOD	Ref
AFP	GCE	CPPPPEKEKEKEK	NH_2	PANI	DPV	0.1 fg mL^{-1}–1 ng mL^{-1}	0.03 fg mL^{-1}	[87]
Cyclin A2	GCE	RRLIFGGGGG/ FHLALYTVT-GQSWPESLIRK-TGYTLESLKP-CLMGGGGG	—♠	Pt NPs/palladium nanocages	ECL	0.001–100 ng mL^{-1}	0.3 pg mL^{-1}	[92]
miRNA 410	PGE	FF	—♠	Au NPs	EIS	10 fM–300 pM	3.90 fM	[91]
miRNA-192	PGE	FF	—♠	GO	EIS	10 fM–1 nM	8 fM	[89]
Breast stem cancer cells	GE	KLVFFGGRLVSYN-GIIFFLK	Dibenzocyclooctyne-amine (DBCO-NH_2)	Multifunctional nanofibers/Ag NPs	LSV	10–5×10^5 cells mL^{-1}	6 cells mL^{-1}	[93]
K562 cancer cells	GCE	FF	NH_2	PNT	EIS	5×10^3–5×10^7 cells mL^{-1}	630 cells mL^{-1}	[94]
Apoptotic HL-60 cells	Indium-tin oxide (ITO) electrode	FNFRLKAGAKIRF-GRGC	NH_2	Hollow TiO_2 Spheres/ reduced graphene (rG)/$ZnIn_2S_4$ nanocrystals	PEC	1×10^3–5×10^7 cells mL^{-1}	158 cells mL^{-1}	[95]
Carcinoembryonic antigen (CEA)/ PSA	Au-Paper Electrode	CEHSSKLQLAK	NH_2	Cyclodextrin functionalized Au NPs (CD@Au NPs)/Au NPs	DPV	CEA: 0.005–100 ng mL^{-1}; PSA: 0.002–40 ng mL^{-1}	CEA: 0.002 ng mL^{-1}; PSA: 0.001 ng mL^{-1}	[96]
PSA	GE	CGGHSSKLQFW-YFWY	Thiol	GO/Ag NPs	LSV	5–2×10^4 pg mL^{-1}	0.33 pg mL^{-1}	[97]
PSA	CdTe/TiO_2 electrode	CEHSSKLQLAK	NH_2	QDs film/TiO_2 nanotubes	PEC	0.005–20 ng mL^{-1}	0.0015 ng mL^{-1}	[40]
PSA	PGE	FF	—♠	PNT/Au NPs/PANI composite (PANI/ AuNP-PNT)	CA	1–100 ng mL^{-1}	0.68 ng mL^{-1}	[98]
PSA	Carbon screen-printed carbon electrode	HSSKLQ	Biotin	Au NPs	DPASV	0.1–100 ng mL^{-1}	27 pg mL^{-1}	[99]
PSA	GCE	ATCUN	NH_2	Carbon nanotube (CNT)/GO	LSV	10 pg mL^{-1}–2 ng mL^{-1}	10 pg mL^{-1}	[100]
PSA	GCE	CEHSSKLQLAK	NH_2/ Thiol	Fe_3O_4@Au magnetic nanocomposites/ multi-walled carbon nanotubes (MWCNTs)	DPV	0.001–30 ng mL^{-1}	0.78 pg mL^{-1}	[101]
PSA	GCE	CGGGGMERCPIK-MFYNLGSPYMNI	—♠	Au@PDA@BCN nanocomposite/ AuPt@MnO_2@ COF nanocomposite	DPV	0.00005–10 ng mL^{-1}	16.7 fg mL^{-1}	[85]

Table 2 (continued)

Analyte	Signal transducer	Peptide	Functional group interacted with peptide sequence	Nanomaterial (s)	Detection technique (s)	Detection range	LOD	Ref
PSA	GCE	CEHSSKLQLAK	NH_2	MWCNTs–(poly(amidoamine) dendrimers) PAMAM/dithiobis(succinimidylpropionate) (DSP)@Au@SiO_2 nanohybrids	LSV	0.001–30 ng mL^{-1}	0.7 pg mL^{-1}	[102]
PSA	GCE	Silk peptide	NH_2	rGO	DPV	5–80 ng mL^{-1}	53 pg mL^{-1}	[103]
PSA	GCE	CEHSSKLQLAK	NH_2	Au NPs	EIS	0.2 pg mL^{-1}–45 ng mL^{-1}	0.06 pg mL^{-1}	[104]
PSA	GCE	CEHSSKLQLAK	NH_2	Chitosan/GO	SWV	1 fg mL^{-1}–100 ng mL^{-1}	1 fg mL^{-1}	[105]
PSA	GCE	CAAAHHHHH-HHSSKLQ	Hemin/G-quadruples	Polyethyleneimine-reduced graphene oxide@hollow platinum nanotubes (PEI-rGO@PtNTs) nanocomposites	DPV	5 mL^{-1}–20 ng mL^{-1}	2 fg mL^{-1}	[106]
PSA	GCE	HSSKLQ	Thiol	Au NPs/$MoSe_2$@rGO nanocomposite	DPV	1 fg mL^{-1}–80 ng mL^{-1}	0.3 fg mL^{-1}	[84]
PSA	ITO	KQLKSSHDKKDK-DPPPPC/ FCDKD-KDKDPPPPC	NH_2/ Thiol	Au NPs/GO-Fe_3O_4-thionine (Thi) nanocomposite	DPV/ CA	5 pg mL^{-1}–10 ng mL^{-1}	DPV: 0.76 pg mL^{-1} CA: 0.42 pg mL^{-1}	[107]
MMP-7	GCE	RPLALWRSCCC	Biotin/ Thiol	Magnetic nanoprobe	SWV	0.1 pg mL^{-1}–50 ng mL^{-1}	0.02 pg mL^{-1}	[108]
MMP-7	GCE	KKKRPLALWR-SCCC	NH_2/ Thiol	Au NPs/Pt NPs	DPV	0.2 pg mL^{-1}–20 ng mL^{-1}	0.05 pg mL^{-1}	[109]
MMP-7	GCE	KKKRPLALWR-SCCC	NH_2/ Thiol	Pd-functionalized carbon Nanocomposites	SWV	100 fg mL^{-1}–100 ng mL^{-1}	17.38 fg mL^{-1}	[110]
MMP-7	GCE	KKKRPLALWR-SCCC	NH_2/ Thiol	Pd NPs/Au-rGO nanocomposite	SWV	10 fg mL^{-1}–10 ng mL^{-1}	3.1 fg mL^{-1}	[111]
MMP-2	GE	FGPLGVRGKGGC/ FGGGASLW-WSEKL	Cucurbit[8]uril (CB[8])	Ag NPs	SWV	0.5 pg mL^{-1}–50 ng mL^{-1}	0.12 pg mL^{-1}	[82]
MMP-2	GCE	KGRVGLPGC	NH_2	Au@Pt nanorods	DPV	0.5–100 ng mL^{-1}	0.18 ng mL^{-1}	[83]
MMP-2	GCE	GGKGRVGLPGC	NH_2/ Thiol	Au NPs/rGO/Pt NPs	SWV	0.01 -10 ng mL^{-1}	–-*	[112]
MMP-2	GCE	GPLGVAGLGGC	Biotin	Au NPs/Pt NPs	DPV	1 pg mL^{-1}–10 ng mL^{-1}	0.32 pg mL^{-1}	[113]

Table 2 (continued)

Analyte	Signal transducer	Peptide	Functional group interacted with peptide sequence	Nanomaterial (s)	Detection technique (s)	Detection range	LOD	Ref
MMP-2	GCE	GGKGRVGLPGC	Thiol	Pb^{2+} loaded carbon spheres (CS)-Au NPs nanocomposites (CS-Au NPs-Pb^{2+})	SWV	1 pg mL^{-1}–1 μg mL^{-1}	0.40 pg mL^{-1}	[114]
MMP-2	GCE	KKKPLGVRGCCC	NH_2/ Thiol	Au NPs	DPV	0.5 pg mL^{-1}–50 ng mL^{-1}	0.15 pg mL^{-1}	[115]
MMP-2	GCE	GPLGVRGKGGC	Biotin	Pt–Pd- mesoporous-hollow ceria nanospheres (Pt–Pd- mhCeO$_2$NS)	DPV	0.1 pg mL^{-1}–10 ng mL^{-1}	0.078 pg mL^{-1}	[116]
Tumor exosomes	GCE	FNFRLKAGAKIRF-GRGC	Thiol	Au NFs/Au NPs@g-C_3N_4 nanocomposite	ECL	1×10^2–1×10^7 particles μL^{-1}	39 particles μL^{-1}	[117]

* LOD not reported; ♠ Functional group interacted with the peptide sequence not reported or not applicable.

and 0.25 mM $HAuCl_4$. It should be considered that the peptide Lum-Au NPs@g-C_3N_4 nanoprobe was obtained via several steps. Initially, Lum (as the chemiluminescent compound)-Au NPs@g-C_3N_4 nanocomposite (ECL signal agent) was synthesized through the electrostatic interaction between a mixture of positively charged g-C_3N_4 nanosheets and a negatively charged solution containing Lum-Au NPs. Then, the peptide was added and could create the Au–S covalent bond between the thiol group of peptide and nanogold molecules. Also, BSA solution was used to block unwanted active sites of the peptide on the surface of the presented electrode. The ECL measurements were followed in a solution containing PBS and H_2O_2. The g-C_3N_4 nanosheet showed catalytic activity in the breakdown of H_2O_2 to OH molecules. So, in the presence of the analyte, the ECL signal was enhanced. This biosensor could detect the PS exosomes in a linear range from 1×10^2–1×10^7 particles μL^{-1}, and the reported LOD was 39 particles μL^{-1}. Immunoglobulin G (IgG), as the most accessible antibody in circulation, has been detected in a peptide-based biosensor using a GCE modified first with polymer poly (3,4-ethylene dioxythiophene) (PEDOT)-citrate as an enhancing agent for electron transfer and then was modified with Au NPs through an electrodeposition method [119]. The synthesis solution of Au NPs consisted of 0.5 mM $HAuCl_4$ and 0.5 M KNO_3. The electrodeposition process was processed via 4 times CV in a potential range from − 1500 to 500 mV. The biorecognition element of this biosensor was a Y-shaped peptide with a sequence (CPPPPEK (HWRGWVA) EKEKEKE) containing two branches. The part of EKEKEKE was applied as antifouling, while HWRGWVA was directed for detecting the analyte (IgG). The mentioned peptide was successfully immobilized on the surface of the working electrode (modified with PEDOT/Au NPs) through interactions created by the Au–S bond. Here, the three-electrode system was used where the other two electrodes, including counter and reference, were platinum and saturated calomel electrodes, respectively. It should be noted that $[Fe(CN)_6]^{3-/4-}$ was applied as the redox marker in the electrochemical measurements. In the presence of IgG molecules, due to the high affinity of peptide sequences against analyte, most of the analyte molecules were captured by the biorecognition element. The accumulation of analyte molecules on the electrode hampers the access of redox marker molecules to the surface of the working electrode; so, along with increasing the concentration of analyte, the DPVs peak current was reduced regularly. Using the DPV technique, this signal-off biosensor could detect IgG in a linear range from 100 pg mL^{-1} to 10 μg mL^{-1}, and the reported LOD was about 32 pg mL^{-1}. Determining the exact value of this biomarker and comparing it with the reference range (6–16 g L^{-1}) can be applied to diagnose some autoimmune and viral diseases. Dopamine is an essential messenger in the brain

with many functions that affect motivation, memory, attention and even regulation of body movements [120]. Dopamine deficiency can cause many problems such as depression, Parkinson's disease, schizophrenia, and addiction. Excessive dopamine level causes euphoria, aggression, and intense sexual feelings. In a research, a peptide-based biosensor has been introduced to diagnose dopamine as an essential neurotransmitter [121]. Here, a nanofibrous peptide hydrogel as the biorecognition element was synthesized in a solvent-switch method via a peptide sequence (FEKF), and the N-terminal of this peptide had a modification with the fluorenylmethoxycarbonyl group. In order to design the biosensing platform, a GCE was used as the working electrode, while the counter and reference electrodes were platinum and saturated calomel, respectively. The surface area of the working electrode was modified with peptide hydrogel and Au NPs. The nanoparticles were synthesized by a hydrothermal method (reduction of $HAuCl_4$ by sodium citrate). The reported size of these nanoparticles was about 15–20 nm (characterized by TEM). In the presence of dopamine, the applied peptide hydrogel could catalyze this neurotransmitter into dopamine quinone. The role of Au NPs was enhancing the electrode area and also electrocatalytic activity when dopamine was converted to dopamine quinone. The electrochemical measurements were performed using DPV, and this signal-on biosensor could diagnose dopamine in a linear concentration range (0.1–10 μM) while the LOD was reported as 21 nM. It should be noted that the produced peptide hydrogel also was applied in interaction with Au NPs and ciprofloxacin as a novel antibacterial agent against several bacteria, including *P. aeruginosa*, *S. aureus*, and *E. coli*, in the solid and liquid culture mediums [121]. Alzheimer's disease (AD) is a neurodegenerative disorder characterized by cognitive problems such as learning and memory deficits. Amyloid-β (Aβ) is the primary biomarker for diagnosing AD [122]. In a study, our team developed a peptide-based biosensor using the modified GE with microporous gold nanostructure to create an electrochemical diagnostic tool against Aβ [44]. Firstly, the microporous gold nanostructure was synthesized on the surface of the GE using a solution containing a mixture of 20 mM $HAuCl_4$, 150 mM sodium alendronate (as the shape directing and size controlling agent), and 500 mM H_2SO_4. The electrodeposited gold nanostructure on the electrode surface showed irregularly shaped deposits with the size of 150 × 250 nm were characterized by SEM. Then, a thiol functionalized peptide (CPPPPTHSQWNKPSKPKTNMK) was immobilized on the surface of the working electrode as the biorecognition element. Here, before the immobilization of the biorecognition element on the surface of the gold nanostructure, the S–S bond between peptide molecules was broken by dithiothreitol (DTT), and then the whole of added DTT molecules was removed from the peptide stock via ethyl acetate extraction. It should be considered that all transducers have a determined optimization time for to be treated with the biorecognition element molecules; after considering this time, the further immobilization and also the unwanted immobilization of the biorecognition element should be blocked (here, the blocking process was performed by MCH). The electrochemical measurements for Aβ detection were followed by the DPV technique in a solution containing $[Fe(CN)_6]^{3-/4-}$ as the redox marker and the counter and reference electrodes were platinum and Ag/AgCl respectively (for the applied three-electrode system). When the biosensor was in the presence of various concentrations of analyte, the molecules of the biorecognition element could capture the analyte, and the electron transfer rate was reduced due to the accumulation of bound analyte molecules on the surface of the transducer. This signal-off biosensor reported a linear detection range, from 3 to 7000 pg mL^{-1}, and the obtained LOD was 0.2 pg mL^{-1}. When the coronary arteries are blocked, enough oxygen will not be reached to the myocardial tissue, and the cells of this vital muscle will be damaged irreversibly. Troponin, as an important protein, is released into the bloodstream from damaged cells. This protein has three subunits, including troponin I (TnI), troponin T (TnT), and troponin C (TnC) [123]. TnI is the gold standard biomarker for the early diagnosis of myocardial infarction. Our team reported a peptide-based biosensor to determine different concentrations of TnI using a modified GE with triangular icicle-like gold nanostructure [24]. Herein, a three-electrode system was applied wherein the gold, platinum, and Ag/AgCl electrodes were used as working, counter, and reference, respectively. The gold nanostructure was synthesized via a solution containing 20 mM $HAuCl_4$, 150 mM vitamin B6 (shape-directing and size-controlling agent), and 500 m MH_2SO_4. The size of the achieved icicle-like gold nanostructure on the surface of the working electrode was about 50 nm (characterized by SEM). The working electrode was modified with a layer of the mentioned icicle-like gold nanostructure through an electrodeposition procedure (chronoamperometry, potential: 0 mV, time: 300 s) (Fig. 5). At the next step, a thiol functionalized peptide sequence (FYSHSFHENWPSC) utilized as the biorecognition element was immobilized on the surface of the modified GE with the gold nanostructure. During the immobilization of the biorecognition element on the surface of the gold nanostructure, a covalent bond was established between the thiol group of cysteine (C) residue of peptide and gold molecules. Finally, to block the unwanted active site of the peptide on the surface, the working electrode was treated with MCH. The prepared biosensor was applied to determine various concentrations of the analyte. The electrochemical measurements were performed using the DPV technique and in the presence of a fixed concentration of $[Fe(CN)_6]^{3-/4-}$ used as the redox marker. In the presence of the

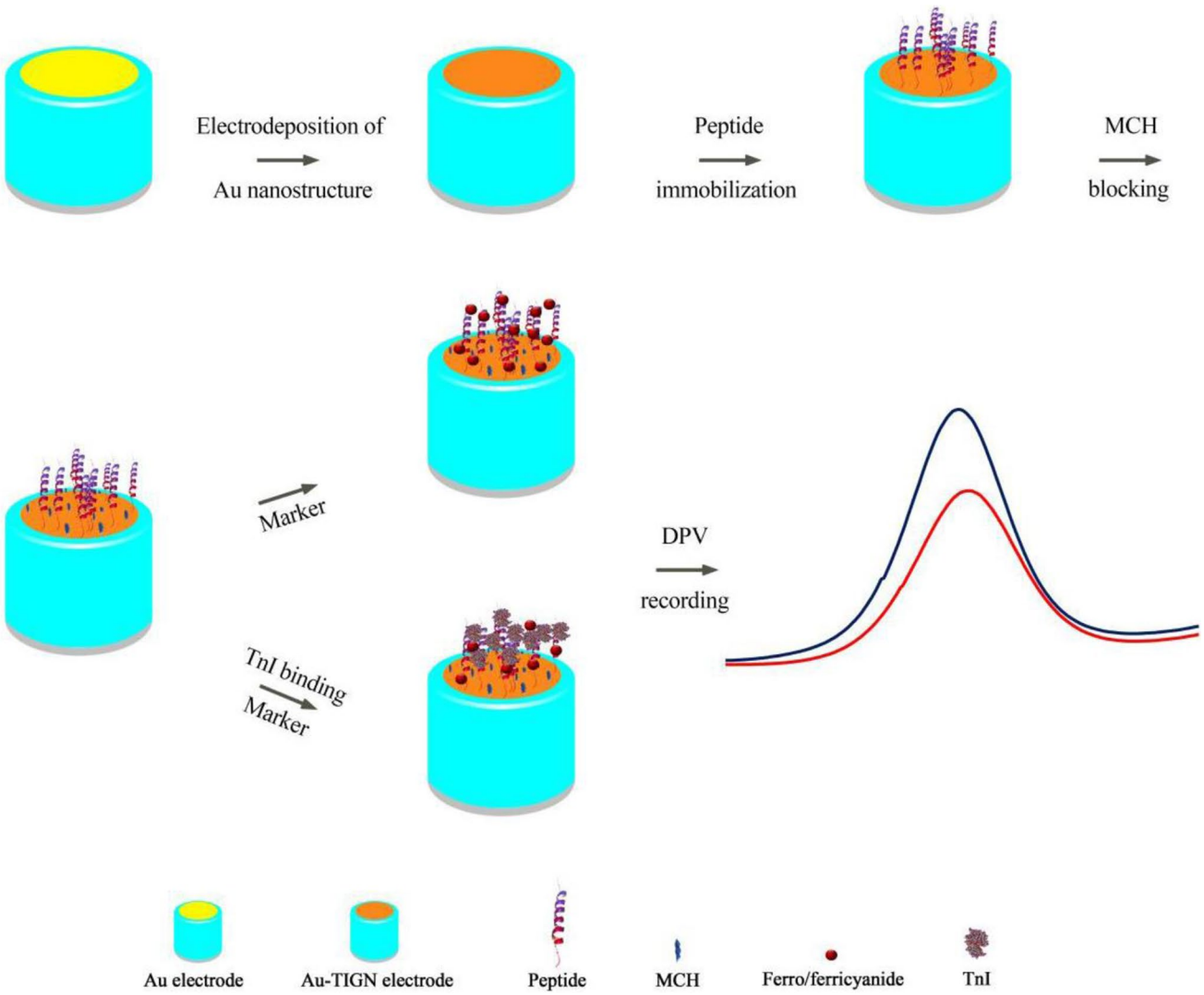

Fig. 5 A peptide-based biosensor for detection of TnI; a modified GE with icicle-like gold nanostructure as the transducer and a peptide sequence as the biorecognition element; permission number: 5105630992928

analyte, due to the high affinity of the biorecognition element, most of the analyte molecules were captured, and the access of the redox marker to the electrode surface was restrained by these analyzed molecules (Fig. 5). This mechanism was led to reduce the electron transfer rate and subsequently decrement the DPV peak current along with enhancement of the analyte concentrations. The presented signal-off biosensor could detect the various concentrations of TnI in a linear range from 0.01 to 5 ng mL^{-1} while the LOD was about 0.9 pg mL^{-1}.

Rituximab is used as a drug (chimeric monoclonal antibody) to treat acute lymphatic diseases such as chronic lymphocytic leukemia, small lymphocytic lymphoma, diffuse large B-cell lymphoma, nodular lymphocyte-predominant Hodgkin lymphoma, follicular lymphoma, mantle cell lymphoma, lymphoblastic lymphoma, and Burkitt lymphoma. In addition, this drug is also used to treat anemia (autoimmune Hemolytic anemia and Hemophilia A) [124]. Rituximab in lymphoma patients' plasma was detected as the analyte by a peptide-based biosensor designed through a modified GE with poly adenine ($polyA_n$) DNA sequence and a peptide sequence in a relationship with a specified antibody (Ab) labeled with Au NPs [125]. First, the surface of the GE was equipped with a peptide (CN14: CGSGSGSWPRWLEN) and an anti-fouling polyAn DNA sequence (polyA20). On the other side, a specified antibody labeled with Au NPs (average size diameter: 13 nm) was prepared. Au NPs were applied as the signal amplifier, and the prepared antibody indicated a high affinity to capture the Fc region of Rituximab. In this case, the modified GE with CN14/polyA20 was immersed in the analyte solution and then incubated at room temperature. Finally, the antibody labeled with

Au NPs was added on the surface of the electrode, and the electrochemical measurements were followed via the EIS technique in the presence of $[Fe(CN)_6]^{3-/4-}$ as the redox marker. The EIS evaluations for this sandwich assay platform showed that the minimum Rct against the bare GE and the Rct was increased for GE/CN14, GE/CN14/polyA20, GE/CN14/polyA20/ Rituximab, and GE/CN14/polyA20/ Rituximab/Ab/Au NPs steadily. The enhancing Rct value was related to reducing the electron transfer rate between the redox marker molecules and the transducer. This biosensor detected Rituximab in a range from 0.1 to 50 μg mL^{-1}, and the calculated LOD was about 35.26 ng mL^{-1}. Trypsin is an enzyme secreted by pancreatic cells as a proenzyme that helps digest proteins. This enzyme is endopeptidases, so it breaks down proteins into polypeptides. This enzyme is secreted from the pancreas [126]. Accurate detection of this enzyme is applicable in diagnosing renal failure and pancreatic tumors. A novel peptide-based ECL biosensor has been introduced to detect trypsin using a copper-based metal–organic framework (JUC-1000) as an ECL emitter [127]. Here, the transducer was a GCE modified with a layer of Au NPs and another nanostructure (core–shell Ag@CeO_2 NPs, size: 40 nm). At the next step, another core–shell structure (JUC-1000-Fe_3O_4@Au-HGC) containing a peptide (HGC) was immobilized on the surface of the mentioned signal transducer (Fig. 6). Finally, to prevent unwanted sites of the biorecognition element from the surface of the signal transducer, the BSA was added, and then the prepared biosensor was applied to determine various concentrations of trypsin. The ECL measurements were followed in a PBS solution containing $S_2O_8^{2-}$ as the redox marker. Electrochemical catalytic behaviors were related to reducing $S_2O_8^{2-}$ to sulfate anion radicals ($SO4^{\bullet-}$). The presence of trypsin as the analyte was led to the cleavage of HGC polypeptide from the carboxyl side of arginine residues (Fig. 6). This event was led to removing the JUC-1000 from the surface of the signal transducer and subsequently decreasing the ECL responses along with increasing the concentrations of the trypsin gradually. The presented signal-off biosensor could detect trypsin in a linear range from 10 fg mL^{-1} to 100 ng mL^{-1}, and the reported LOD was 3.46 fg mL^{-1}.

Lipopolysaccharides (LPS) are large molecules also known as lipoglycans and endotoxins. These molecules are found in the outer membrane of Gram-negative bacteria, which produce robust immune responses in humans, such as septic in the blood circulation [128]. Yang et al. developed a peptide-based impedimetric biosensor for the diagnosis of LPS (from *Escherichia coli* O55:B5) [129]. Electrochemical measurements were followed using a three-electrode system (a GCE as the working, a platinum wire as the counter, and a saturated calomel electrode as the reference). The $[Fe(CN)_6]^{3-/4-}$ was used as the redox marker during electrochemical studies. In order to design the LPS biosensor, initially, the surface of the GCE was modified with a solution containing TiO_2, 5,10,15,20-Tetrakis(4-aminophenyl)-21H,23H-porphine (TAPP), and Nafion-ethanol.

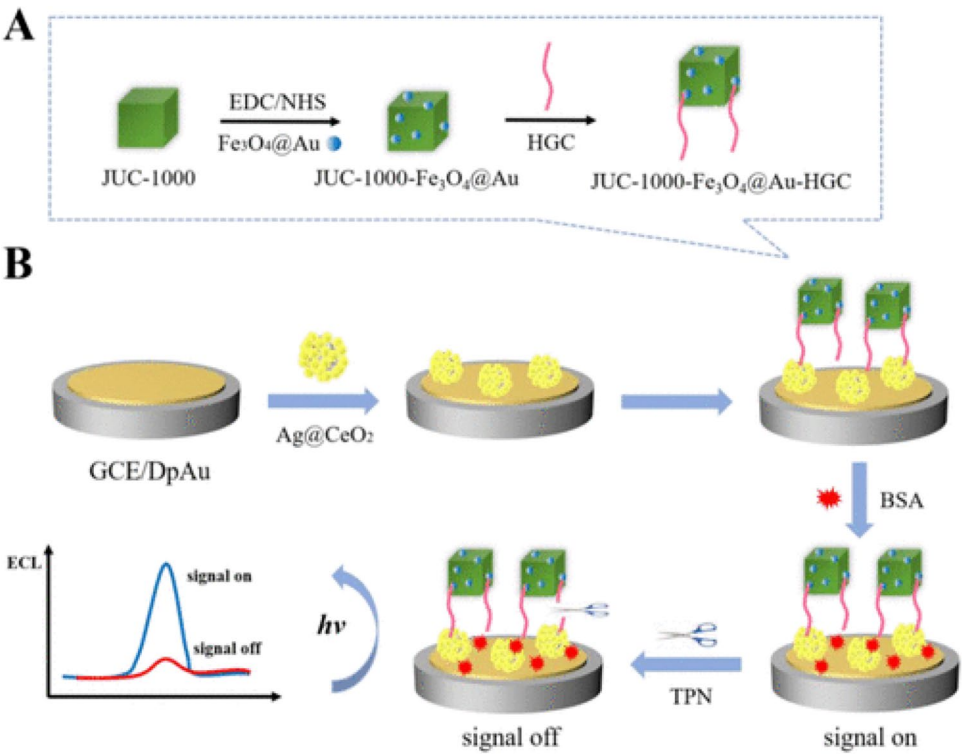

Fig. 6 An ECL peptide-based biosensor for detection of trypsin; a modified GCE modified with a layer of Au NPs as the transducer that was applied along with the presence of JUC-1000-Fe_3O_4@Au-HGC) containing a peptide (HGC); permission granted by American Chemical Society

Subsequently, the (colloidal) Au NPs were dropped on the surface of modified GCE with TiO_2 and TAPP, and the final form of the signal transducer was obtained. Afterward, the biorecognition element (Li5-025 peptide (KYSSSISSIRAC)) was immobilized on the surface of the presented GCE, and the achieved peptide-based biosensor was applied for the determination of the various concentrations of LPS. The analyte detection was followed via the EIS technique, and the Ret was increased along with enhancing the concentrations of LPS. It seems, in order to the high affinity between the biorecognition element and the analyte molecules, the electrostatic repulsion was increased between the analyte and redox marker molecules, and the steric hindrance of the biorecognition element/analyte complex was also enhanced. The mentioned mechanism can be considered for enhancing Ret during impedimetric measurements when the biorecognition element captured the analyte. The linear detection range against LPS in serum samples has been reported as 0.1 pg mL^{-1} to 100 ng mL^{-1} with a LOD of about 0.08 pg mL^{-1}. Protein kinase is an essential group of enzymes that phosphorylates proteins by adding the phosphate group. Unusual expression of these enzymes has been found in some diseases, especially Alzheimer's disease and cancers [130]. A PEC peptide-based biosensor was developed to detect protein kinase A using a modified ITO electrode with Au NPs [131]. In this PEC biosensor, the ZrO_2/CdS octahedral nanocomposite (5.62 nm) as a part of the biosensing platform was produced by calcination (500 °C) of zirconium-based metal–organic frameworks (UiO-66) and then modification with CdS nanoparticles (Fig. 7). Here, the surface of the ITO electrode was modified with Au NPs (characterization by SEM: average size diameter: 35 nm) through an electrodeposition method (5 times CV, potential: − 900–500 mV, scan rate: 50 mV s^{-1}). Subsequently, a peptide sequence (LRRASLGGGGC) as the biorecognition element was immobilized on the surface of the ITO. The peptide strands were anchored on the Au NPs through the cysteine residue, and the unwanted and non-specifically binding sites of them were blocked by MCH molecules. At the next step, the analyte solution containing a mixture of protein kinase A and adenosine triphosphate (ATP) was dropped on the surface of the modified electrode.

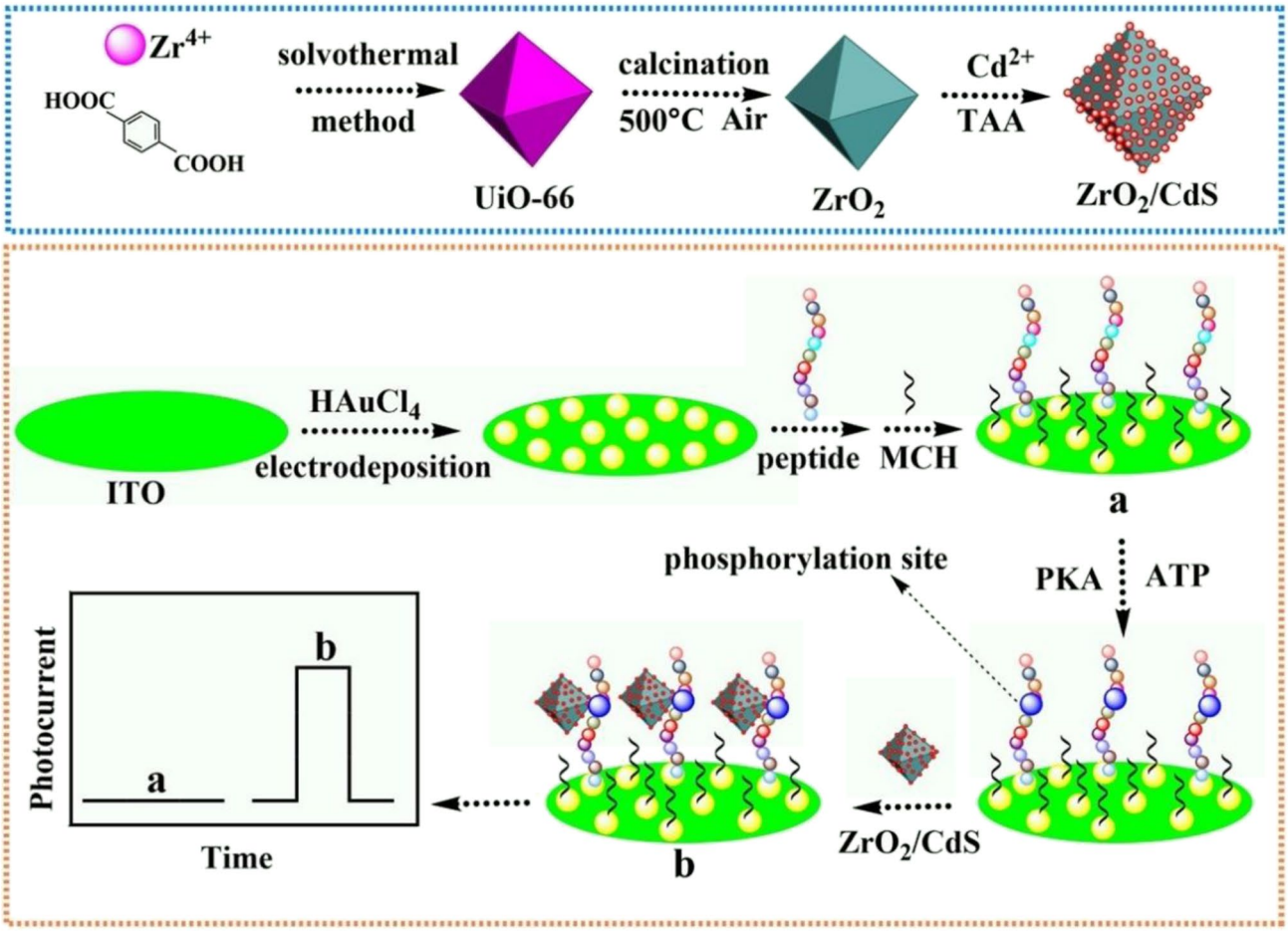

Fig. 7 A PEC peptide-based biosensor to detect protein kinase A; permission number: 5223271447069

At this moment, the analyte molecules were captured by the peptide strands, and the used ATP molecules directed the phosphorylation of serine (S) residue in peptide sequence by the analyte. Finally, the prepared ZrO_2/CdS octahedral nanocomposite was added to the surface of the electrode, and it could be bound with the phosphorylated area of peptide due to the high affinity between ZrO_2 molecules and the phosphate group of the peptide (Zr-O-P coordination) (Fig. 7). The created anodic photocurrent due to the presented interactions was investigated by UV–Visible spectrophotometry. On the other side, the electrochemical measurements were followed by the EIS technique in a solution containing $[Fe(CN)_6]^{3-/4-}$ as the redox marker, where the Rct decreased for the modified ITO electrode with Au NPs and this value was increased after immobilization of the biorecognition element, analyte and also adding ZrO_2/CdS octahedral nanocomposite, regularly. The increase of Rct was due to enhancing the electrostatic repulsion action of the redox marker ions on the surface of the transducer. The linear detection range for the mentioned PEC peptide-based nanobiosensor was 0.001 to 100 U mL^{-1}, and the reported LOD was 0.00035 U mL^{-1}.

In Table 3, the main features of electrochemical biosensors equipped with peptides and nanomaterials that their analyte was essential biochemical molecules have been cited.

Analysis of the critical parameters of electrochemical nanobiosensors equipped with peptides

In Fig. 8, the critical features of electrochemical peptide-based biosensors have been evaluated. As mentioned in the introduction of this review, the signal transducer is the essential component of biosensors that convert the signal received by the biorecognition element into an analyzable signal. As shown in Fig. 8(a), the primary signal transducers used in the design of peptide biosensors in recent years include GCE (53%), GE (25%), and ITO (7%). In the design of these biosensors, the source substance of the signal transducer and the type of the biorecognition element (especially functional groups) had a compatible relationship. This relationship is based on an efficient connection between the signal transducer and the biorecognition element since the desired interactions are only possible with certain chemical bonds. Other factors influencing the choice of a signal transducer include simple modification, reasonable manufacturing cost, stability, and high sensitivity in the electron transfer process. In Fig. 8(b), the main techniques used in the process of electrochemical detection of analytes have been analyzed. Among all the electrochemical peptide-based biosensors studied, the main diagnostic techniques used were DPV (35%), EIS (19%), and SWV (16%), respectively. The most important reasons for choosing any diagnostic technique are considering the best diagnostic sensitivity, compatibility with the signal marker, finding desired LOD, electrolyte compatibility, optimum analyte detection time, and providing more detailed outputs. The use of nanomaterials in biosensors is generally aimed to accelerate and facilitate the immobilization processes of the biorecognition element and improve the analyte detection processes. Nanomaterials increase the diagnostic sensitivity of biosensors and accelerate the analyte detection process due to the increased diagnostic active area, so as due the electrocatalysis proportionated by these nanomaterials. Figure 8(c) presents the main nanomaterials used in the reviewed electrochemical peptide-based biosensors. As it turns out, most of the nanomaterials used in the design of electrochemical peptide-based biosensors include Au nanostructures (28%), carbon-based nanomaterials/their derivatives (16%), and Au nanocomposites (13%). The use of any nanostructure generally depends on the type of signal transducer, the type of interaction with the biorecognition element, biocompatibility, the enhanced rate of the diagnostic sensitivity, the cost of production, and the ease of use (deposited or conjugated). One of the most important bridges between the biorecognition element and the signal transducer is the use of functional groups such as thiol, amine, carboxyl, and biotin. In most of the reviewed electrochemical peptide-based biosensors, peptide sequences were used as the main biorecognition element. However, in some cases, these peptide sequences were applied as a part of a biorecognition element along with antibodies, aptamers, etc., to facilitate the analyte detection process. In Fig. 8(d), the functional groups interacting with the peptide sequences have been listed. The most important functional groups in interaction with peptide sequences were thiol (43%), amine (31%), and biotin (12%), respectively. The use of any functional group in interaction with peptide sequences depends on compatibility and optimal binding with the signal transducer or other parts of the biorecognition element. In most cases, peptides were immobilized and used directly on the surface of the signal transducer (86%). However, in some cases, these peptide sequences were associated with other components of the biorecognition element and were not directly in interaction with the surface of the signal transducer (Fig. 8(e)). Peptides are formed by covalent bonds created between the carboxyl group of one amino acid and the amino functional group of another amino acid. The maximum number of participating amino acids in peptide sequences is 50. Amino acids are organic compounds that consist of an amine group ($-NH_2$), a carboxyl group (-COOH), an alkyl group as a side chain (-R), and a hydrogen atom (-H). Thus, an amino acid comprises four basic chemical elements, including hydrogen, oxygen, nitrogen, and carbon [34, 162]. Peptide sequences have recently been used in the structure of biosensors as the biorecognition

Table 3 Main features of electrochemical biosensors equipped with peptides and nanomaterials designed for diagnosing essential biochemical molecules

Analyte	Signal transducer	Peptide	Functional group interacted with the peptide sequence	Nanomaterial (s)	Detection technique	Detection range	LOD	Ref
LPS	GCE	KYSSSISSIRAC	Thiol	Au NPs	EIS	0.1 pg mL^{-1}–100 ng mL^{-1}	0.08 pg mL^{-1}	[129]
LPS	GCE	GIGKLHSAGKF	Thiol	Au NPs	EIS	0.01 pg mL^{-1}–1 ng mL^{-1}	2 fg mL^{-1}	[132]
LPS	GE	CIGKLHSAGK	Thiol	$Ru_1@SiO_2$ NPs	ECL	1–500 ng mL^{-1}	0.3 ng mL^{-1}	[133]
Thioflavin-T	ITO	KLVFFEEEEEE -Y-GSNKGAIIGLM	11-Mercaptoundeca-noic acid	Peptide nano-network	DPV	3.3–3300 pg mL^{-1}	1 pg mL^{-1}	[134]
Dopamine	GCE	FEKF	Fluorene methoxy-carbonyl (Fmoc)	Au NPs	DPV	0.1—10 µM	21 nM	[121]
Aβ	GE	CPPPPTHSQWNKP-SKPKTNMK	Thiol	Microporous gold nanostructure	DPV	3–7000 pg mL^{-1}	0.2 pg mL^{-1}	[23]
Aβ	GE	CTHSQWNKPSKPKT-NMK/ THSQWNKP-SKPKTNMK	Thiol	Ag NPs	LSV	0.01–200 nM	6 pM	[135]
Aβ	GO/GNPs hydrogel electrode	THSQWNKPSKPKT-NMK	Thiol	Au NPs-rGO	EIS	0.1 pM–10 nM	0.1 pM	[136]
Aβ/ Human chorionic gonadotropin (HCG)	GE	Aβ: CTHSQWNKPSK-PKTNMK HCG: CPPLRIN-RHILTR	Thiol	Au NPs	EIS	Aβ: 0.1 nM–0.2 µM HCG: 0.001–0.2 IU mL^{-1}	Aβ: 45 pM HCG: 0.6 mIU mL^{-1}	[137]
HCG	GE	CPPLRINRHILTR	Thiol	Ag NPs	LSV	0.001–0.2 IU mL^{-1}	0.4 mIU mL^{-1}	[138]
HCG	ITO	PPLRINRHILTR/ EKEKEKEPPPPC	NH_2	Au NPs	PEC	0.5–1000 mIU mL^{-1}	0.19 mIU mL^{-1}	[139]
Human growth hormone	GCE	FF	—♠	Flower-like diphe-nylalanine peptide nanostructures (FPNSs)	EIS	1–100 pg mL^{-1}	0.00038 ng mL^{-1}	[140]
DNA- BRCA1	GCE	EKEKEKE	Carboxyl	PEDOT	DPV	1.0×10^{-16} M–1.0×10^{-10} M	0.03 fM	[141]
H_2O_2	GCE	FF	—♠	Nanofibrous hydrogel	CV	0.1–60.2 µM	18 nM	[142]
H_2O_2	GCE	Heme peptide (HP)	—♠	CNTs/graphene	CV	Up to 3×10^{-5} M	—*	[143]
H_2O_2	GCE	FF	—♠	Nanofibrils	CV	7.5×10^{-7}–1.4×10^{-5} M	2.5×10^{-7} M	[144]
Immunoglobulin E (IgE)	GCE	EKEKEKEPPPPC	Thiol	Macroporous Au nanostructure/poly-styrene nanospheres	DPV	0.1–10 pg mL^{-1}	42 fg mL^{-1}	[145]
IgG	GCE	EKEKEKE/ HWRG-WVA	Thiol	Au NPs	DPV	100 pg mL^{-1}- 10 µg mL^{-1}	32 pg mL^{-1}	[119]
Cytomegalovirus pp65 antibody	GCE	CMVpp65 (495–503) Peptide (NLVPM-VATV)	Thiol	SnS_2 QDs/Ag NFs	ECL	1 fM–100 nM	0.33 fM	[146]
Renin	DEP chip	IQRKRQGP	Thiol	Au NPs	DPV	280 µg mL^{-1}–380 ng mL^{-1}	300 ng mL^{-1}	[147]

Table 3 (continued)

Analyte	Signal transducer	Peptide	Functional group interacted with the peptide sequence	Nanomaterial (s)	Detection technique	Detection range	LOD	Ref
TnI	Mercury film modified screen-printed electrode	FYSHSFHENWPS/ GGGAFYSHSFHENWPSK	Biotin	QDs/magnetic beads	DPV	0.001–100 ng mL^{-1}	0.42 pg mL^{-1}	[148]
TnI	GE	CFYSHSFHENWPS	Thiol	Au NPs	ECL	3×10^{-12} g mL^{-1}–7×10^{-11} g mL^{-1}	0.5 pg mL^{-1}	[149]
TnI	GE	FYSHSFHENWPSC	Thiol	Icicle-like gold nanostructure	DPV	0.01–5 ng mL^{-1}	0.9 pg mL^{-1}	[24]
TnI	GCE	CFYSHSFHENWPS	Thiol	Au NPs	EIS	15.5 pg mL^{-1}–1.55 ng mL^{-1}	3.4 pg mL^{-1}	[150]
Trypsin	GCE	CAGRAAADAD	NH_2	$NiCo_2O_4$ nanosheets/ g-C_3N_4 nanocomposite	DPV	10^{-10} – 10^{-4} mg mL^{-1}	10^{-10} mg mL^{-1}	[151]
Trypsin	GCE	HWRGWVC	—♠	Au NPs/Ag@CeO_2 NPs	ECL	10 fg mL^{-1}–100 ng mL^{-1}	3.46 fg mL^{-1}	[127]
Protein kinase A	GCE	CGGALRRASLG-COOH	NH_2/ Carboxyl	Au@C nanocomposite/Au NPs-biotinylated β-galactosidase (B-Gal) nanocomposite	DPV	0.05 -100 U mL^{-1}	0.014 U mL^{-1}	[152]
Protein kinase A	GCE	CGGALRRASLG	NH_2/ Thiol	Au NPs	DPV	0.5–25 U mL^{-1}	0.15 U mL^{-1}	[153]
Protein kinase A	ITO	CRRLRRASLG	Thiol	Au NPs/TiO_2/g-C_3N_4 nanocomposite	PEC	0.05–50 U mL^{-1}	0.02 U mL^{-1}	[154]
Protein kinase A	ITO	LRRASLGGGGC	Thiol	Au NPs/ZrO_2-CdS octahedral nanocomposite	PEC	0.001–100 U mL^{-1}	0.00035 U mL^{-1}	[131]
Protein kinase A	GE	TTYADFIASGRTGRRNAIHD	Thiol	Au NPs	DPV	0.01–1 U mL^{-1}	20 mU mL^{-1}	[155]
Thrombin	GE	GHK	—♠	Zirconia nanoparticles (Zr NPs)	SWV	Up to 2000 pg mL^{-1}	0.2 pg mL^{-1}	[156]
Thrombin	GCE	CAAAHHHHHHK	—♠	PtNTs@rGO nanocomposite	DPV	0.05 pM–60 nM	15 fM	[157]
Caspase-3	GE	EEAAADEVDFK-KAAAC	NH_2/ Thiol	Ag NPs	LSV	1–10 ng mL^{-1}	24.62 pg mL^{-1}	[158]
Caspase-3	GCE	GDGDEVDGC	Biotin	Au NPs-rGO	ECL	0.5–100 fM	0.5 fM	[159]
Caspase-3	GCE	GDGDEVDGC	Biotin	Au NPs	SWV	10 fM -10 nM	5 fM	[160]
Caspase-3	GCE	GDEVDSKFFFF	NH_2/ Carboxyl	GO	CV	0.5 pg mL^{-1}–2 ng mL^{-1}	0.2 pg mL^{-1}	[41]

Table 3 (continued)

Analyte	Signal transducer	Peptide	Functional group interacted with the peptide sequence	Nanomaterial (s)	Detection technique	Detection range	LOD	Ref
Poly(ADP-ribose) polymerase-1 (PARP-1)	GCE	CCYGGVLRR	NH_2/ Thiol	Cu NPs	DPV	0.01 U–1U	0.004 U	[161]
Rituximab	GE	CGSGSGSWPRWLEN	—♠	Au NPs	EIS	0.1–50 µg mL^{-1}	35.26 ng mL^{-1}	[125]

* LOD not reported; ♠ Functional group interacted with the peptide sequence not reported or not applicable.

element or as part of a biorecognition element component. Proper selection of the peptide sequences and optimal and controlled synthesis of them based on diagnostic aims has a great impact on the sensitivity, selectivity, and stability of biosensors. Regarding the mission of peptides in the structure of biosensors, these macromolecules can interact with their targets by folding and changing conformations. One of the important diagnostic principles regarding the application of peptides in the structure of electrochemical biosensors is the changes in the electron transfer rate of their molecular interactions with other components of biosensors. Due to this important point, these peptides can specifically reflect these molecular interactions quantitatively through changes in the rate of electron transfer. In this review, it was found that in recent researches, the presence of analytes and the establishment of interactions with peptide sequences have been associated with changes in electrical current as well as changes in electrical resistance on the surface of signal transducers. Due to the possibility of designing and synthesizing peptide sequences by considering their analytes, the selectivity of peptide biosensors has been reported at a high level in recent researches. Usually, before synthesizing peptides, the optimal state is considered in terms of temperature, chemical, and structural stability. Other biological compounds, such as antibodies and nucleotide sequences, have also been used in the structure of several peptide-based biosensors, which in some cases these biosensors could detect the analyte in a sandwich state. In the reviewed items, on average, all designed peptide-based biosensors reported selectivity of over 90%. One of the most important parameters in successful detection by biosensors is selecting the optimal signal marker. This signal marker should be selected according to the used diagnostic techniques, analyte concentrations, analyte capturing processes by the biorecognition element, and the type of signal transducer. In the review of recent researches in the field of electrochemical peptide-based biosensors, it has been found that the most commonly used signal marker (in electrochemical assays, the signal marker = redox marker) was $[Fe(CN)_6]^{3-/4-}$ (78%). Details of the used signal markers have been provided in Fig. 8(f).

Conclusion

The analytical results of this review showed that researchers are trying to provide new and optimal diagnostic methods (including higher sensitivity, higher selectivity, and lower production costs) using electrochemical biosensors equipped with peptides and nanomaterials. In the reviewed papers, the analysis confirmed that the most common signal transducers used were GCE and GE, respectively. Also, various electrochemical diagnostic techniques have been used in these biosensors, and evaluations showed that the most applied diagnostic techniques

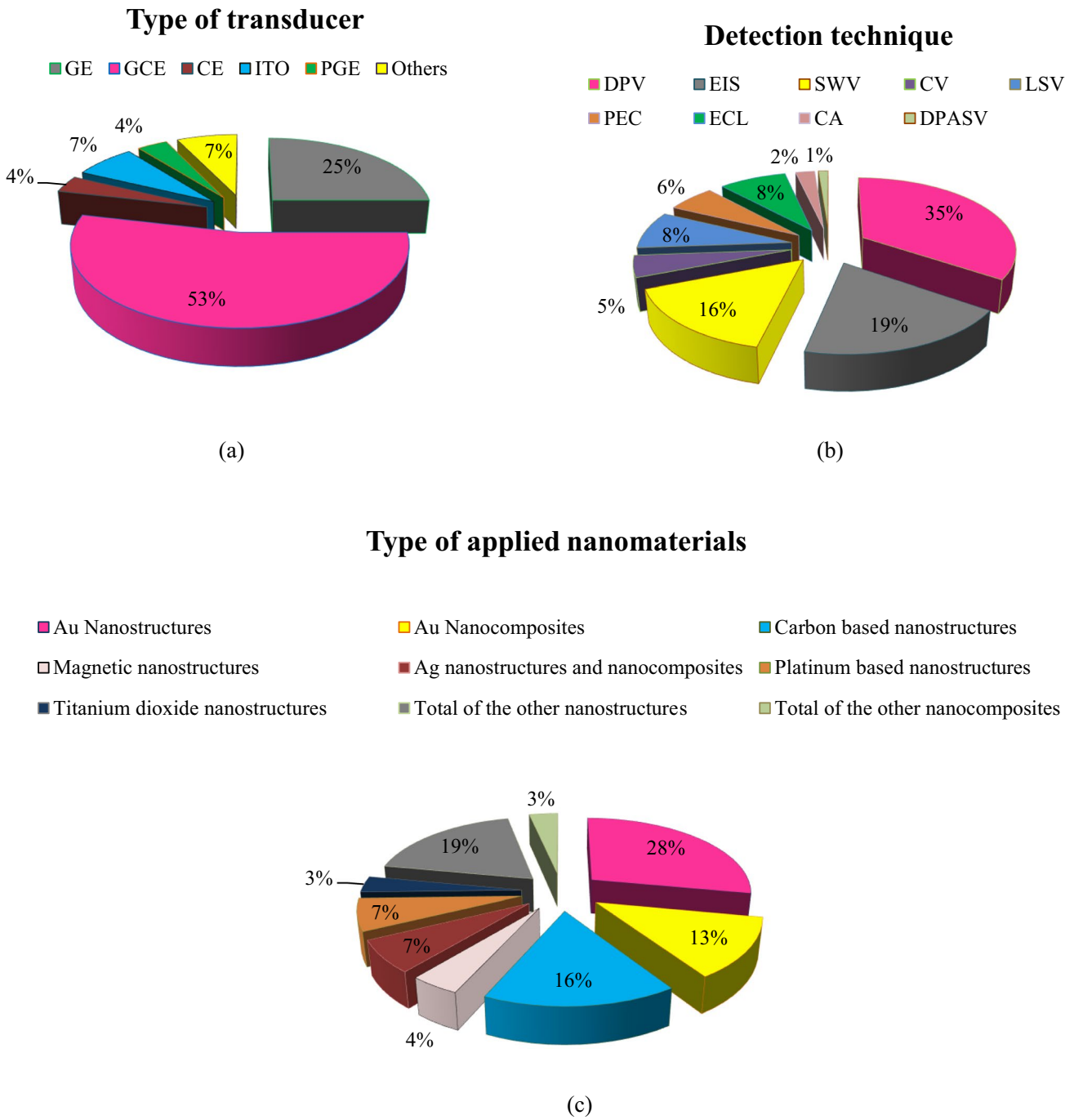

Fig. 8 Analytical features of the recent electrochemical peptide-based biosensors; (**a**) type of the applied signal transducers; (**b**) type of the detection techniques; (**c**) type of the applied nanomaterials; (**d**) various functional groups interacted with the peptide sequences; (**e**) location of peptide sequences against signal transducer, and (**f**) type of the applied signal markers

were DPV, EIS, and SWV, respectively. Applying nanomaterials was led to providing the optimized detection time and also increased the diagnostic sensitivity, which reviewing in recent researches showed that the maximum use was related to gold- and carbon-based nanomaterials. It seems researchers in selecting these nanomaterials have considered higher biocompatibility, easier preparation/use, higher stability, higher diagnostic sensitivity, and production costs. Depending on the surfaces and positions that peptide sequences interacted, different functional groups were used (mostly: thiol, amine, and biotin). For instance, the presence of thiol molecules in the peptide sequences indicates that this sequence can bond well

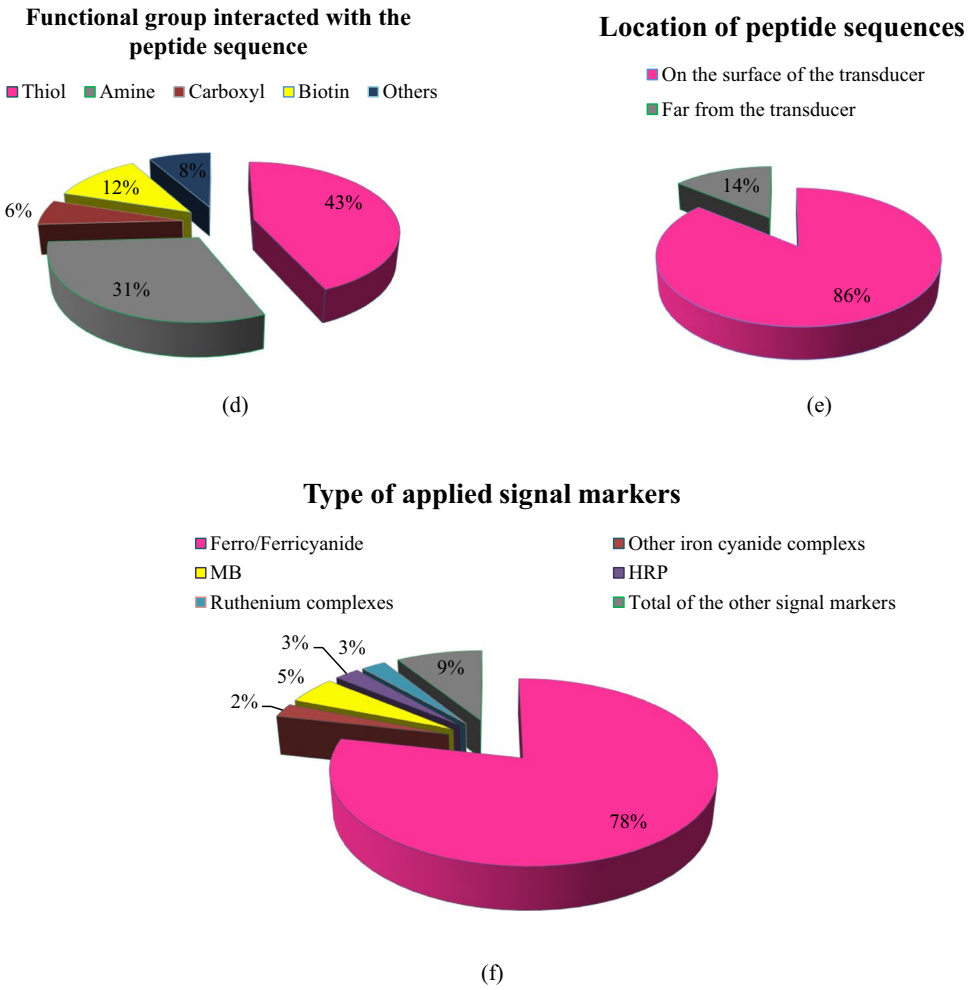

Fig. 8 (continued)

with the gold-based surfaces. For other functional groups, this relationship also exists. In most of the reviewed papers, peptide sequences were directly in contact with the surface of the signal transducer, but in some cases, these peptide sequences were presented in interaction with other parts of the biorecognition element. Finally, it was found that the signal marker in most of the recent researches was $[Fe(CN)_6]^{3-/4-}$, which could reflect an apparent reason for better diagnostic results in comparison with the other signal markers in the evaluated electrochemical peptide-based nanobiosensors. In addition, this signal marker ($[Fe(CN)_6]^{3-/4-}$) is cheap and easy to obtain with the desired purity.

Future perspectives

This review revealed the extraordinary advantages arising from the association of peptides with nanomaterials. The fact that nowadays, it is easy to design and build almost any peptide opens a fantastic road for assembling extremely selective biosensors. The association of these peptides with nanomaterials, which actuates at the same time as the connection point of the peptide with the sensor and as the catalyst of electrochemical reactions with differentiated areas, makes this association extremely effective. The development of these devices will fill an essential gap in the diagnosis in the healthcare area, and the popularization of commercial sensors will happen in the short future. The fast and accurate diagnoses provided by these biosensors will result in lower healthcare costs, and many fields such as industry and environmental chemistry will also be favored. Biosensors present many advantages such as portability, simplicity of use, and relatively low cost. The association of biosensing and voltammetric detection owns the great advantage that involves portability, and in the last decade, the development of wearable sensors dedicated to monitoring some species continuously is gaining popularity. Peptides associated with nanomaterials will find many

applications in this field, not only watching the levels of some species but also examining the appearance of other species that can indicate the starting of some new disease. Relatively, the recognized disadvantages of classical biosensors (narrow ranges of temperature and pH operation), the possibility of engineering new peptides more tolerant to these variations is a real possibility. The association of peptides and nanomaterials opens new opportunities for evolution in the peptide-based biosensing field. One of the most important challenges in the design of biosensors is the requirement to use specific biorecognition elements against each analyte. In fact, the biorecognition elements should be selected with the maximum affinity and specificity to analytes. These peptide-based biorecognition elements must also be in optimal interaction with the signal transducer and also be able to have a successful connection and immobilization in interaction with the other components of the biosensor. Detection of multiple analytes requires the design and application of several specific biorecognition elements against analytes. Also, considering the cost of designing and producing specific peptides in the multiplex mode, the compatibility of all the applied biorecognition elements with other components of biosensors (e.g., signal transducer) should be considered, which can be a complicated mission. Real samples contain analytes and usually include serum, plasma, whole blood, and cells. In addition to the presence of analytes, there are several interfering agents that should not have a significant effect on diagnostic results; this is very important because diseases will be diagnosed according to this type of biosensors in the future, and if the diagnoses provided by biosensors not be accurate enough, the wrong treatment strategies will be adopted, and then the clinical trust in these diagnostic tools will become weak. There are also some limitations related to the stability of peptide biosensors. In this case, the temperature sensitivity of biosensors components is a barrier to the possibility of sterilizing these devices at high temperatures. The effects of pH changes must also be considered. Furthermore, due to the nature of the presence of biological material in biosensors, there are limitations for their storage, use, and lifespan. The market for biosensors is also witnessing a slow commercialization process, primarily due to price sensitivity, end-user acceptance, and concerns about the quality, accuracy, and reliability of products. There are currently few practical systems on the market that play a major role in medical diagnostics. Commercial glucometers are currently the most popular. The cost of building biosensor components must be reasonable and it is not economical on a low-volume scale, but in mass production, which, if it occurs, can undoubtedly be produced at very reasonable and economical costs that can be used as an alternative to existing bioassay systems.

Funding The authors acknowledge the financial support from the São Paulo Research Foundation—FAPESP (Processes 2019/27021–4, 2017/13137–5, 2014/50867–3) and National Council for Research—CNPq (processes 311847–2018-8 and 465389/2014–7).

Declarations

Competing interests The authors declare no competing interests.

References

1. Sezgintürk MK (2020) Commercial biosensors and their applications: clinical, food, and beyond. Elsevier Science
2. Karunakaran C, Bhargava K, Benjamin R (2015) Biosensors and bioelectronics. Elsevier Science
3. Prickril B, Rasooly A (2018) Biosensors and biodetection: methods and protocols, volume 2: electrochemical, bioelectronic, piezoelectric, cellular and molecular biosensors. Springer New York
4. Ensafi AA (2019) Electrochemical biosensors. Elsevier Science
5. Ecker DJ, Sampath R, Massire C, Blyn LB, Hall TA, Eshoo MW et al (2008) Ibis T5000: a universal biosensor approach for microbiology. Nat Rev Microbiol 6(7):553–558
6. Shetti NP, Mishra A, Basu S, Mascarenhas RJ, Kakarla RR, Aminabhavi TM (2020) Skin-patchable electrodes for biosensor applications: a review. ACS Biomater Sci Eng 6(4):1823–1835
7. Lee H, Sun E, Ham D, Weissleder R (2008) Chip–NMR biosensor for detection and molecular analysis of cells. Nat Med 14(8):869–874
8. Du X, Zhang Z, Zheng X, Zhang H, Dong D, Zhang Z et al (2020) An electrochemical biosensor for the detection of epithelial-mesenchymal transition. Nat Commun 11(1):1–9
9. Min J, Sempionatto JR, Teymourian H, Wang J, Gao W (2021) Wearable electrochemical biosensors in North America. Biosensors and Bioelectronics. 172:112750
10. Ren C, Wen X, Mencius J, Quan S (2021) An enzyme-based biosensor for monitoring and engineering protein stability in vivo. Proceedings of the National Academy of Sciences. 118(13)
11. Soylemez S, Kurbanoglu S (2021) Enzyme-based electrochemical nanobiosensors using quantum dots. Electroanalytical Applications of Quantum Dot-Based Biosensors. Elsevier; 307–39
12. Kurbanoglu S, Erkmen C, Uslu B (2020) Frontiers in electrochemical enzyme based biosensors for food and drug analysis. TrAC, Trends Anal Chem 124:115809. https://doi.org/10.1016/j.trac.2020.115809
13. Fang L, Liao X, Jia B, Shi L, Kang L, Zhou L et al (2020) Recent progress in immunosensors for pesticides. Biosensors and Bioelectronics. 164:112255
14. Mansuriya BD, Altintas Z (2020) Graphene quantum dot-based electrochemical immunosensors for biomedical applications. Materials 13(1):96
15. Jia M, Liao X, Fang L, Jia B, Liu M, Li D, et al. (2021) Recent advances on immunosensors for mycotoxins in foods and other commodities. TrAC Trends in Analytical Chemistry. 116193
16. Negahdary M (2020) Aptamers in nanostructure-based electrochemical biosensors for cardiac biomarkers and cancer biomarkers: a review. Biosens Bioelectron 152:112018. https://doi.org/10.1016/j.bios.2020.112018

17. Negahdary M (2020) Electrochemical aptasensors based on the gold nanostructures. Talanta 216:120999. https://doi.org/10.1016/j.talanta.2020.120999
18. Negahdary M, Heli H (2019) An ultrasensitive electrochemical aptasensor for early diagnosis of Alzheimer's disease, using a fern leaves-like gold nanostructure. Talanta 198:510–517
19. Negahdary M, Behjati-Ardakani M, Sattarahmady N, Yadegari H, Heli H (2017) Electrochemical aptasensing of human cardiac troponin I based on an array of gold nanodumbbells-Applied to early detection of myocardial infarction. Sens Actuators, B Chem 252:62–71
20. Negahdary M, Behjati-Ardakani M, Heli H (2019) An electrochemical troponin T aptasensor based on the use of a macroporous gold nanostructure. Microchim Acta 186(6):1–10
21. Taheri RA, Eskandari K, Negahdary M (2018) An electrochemical dopamine aptasensor using the modified Au electrode with spindle-shaped gold nanostructure. Microchem J 143:243–251. https://doi.org/10.1016/j.microc.2018.08.008
22. Heiat M, Negahdary M (2019) Sensitive diagnosis of alpha-fetoprotein by a label free nanoaptasensor designed by modified Au electrode with spindle-shaped gold nanostructure. Microchem J 148:456–466
23. Negahdary M, Heli H (2019) An electrochemical peptide-based biosensor for the Alzheimer biomarker amyloid-β (1–42) using a microporous gold nanostructure. Microchim Acta 186(12):1–8
24. Negahdary M, Heli H (2019) An electrochemical troponin I peptisensor using a triangular icicle-like gold nanostructure. Biochemical Engineering Journal. 151:107326
25. Song D, Zheng J, Myung NV, Xu J, Zhang M (2021) Sandwich-type electrochemical immunosensor for CEA detection using magnetic hollow Ni/C@SiO2 nanomatrix and boronic acid functionalized CPS@PANI@Au probe. Talanta 225:122006. https://doi.org/10.1016/j.talanta.2020.122006
26. Vanova V, Mitrevska K, Milosavljevic V, Hynek D, Richtera L, Adam V (2021) Peptide-based electrochemical biosensors utilized for protein detection. Biosensors and Bioelectronics. 113087
27. Yuan L, Liu L (2021) Peptide-based electrochemical biosensing. Sensors and Actuators B: Chemical. 130232
28. Sfragano PS, Moro G, Polo F, Palchetti I (2021) The role of peptides in the design of electrochemical biosensors for clinical diagnostics. Biosensors 11(8):246
29. Ma F, Zhu Y, Chen Y, Liu J, Zeng X (2019) Labeled and non-label electrochemical peptide inhibitor-based biosensing platform for determination of hemopexin domain of matrix metalloproteinase-14. Talanta 194:548–553. https://doi.org/10.1016/j.talanta.2018.10.057
30. Morales MA, Halpern JM (2018) Guide to selecting a biorecognition element for biosensors. Bioconjug Chem 29(10):3231–3239
31. Asal M, Özen Ö, Şahinler M, Baysal HT, Polatoğlu İ (2019) An overview of biomolecules, immobilization methods and support materials of biosensors. Sensor Review
32. Ladner RC, Sato AK, Gorzelany J, de Souza M (2004) Phage display-derived peptides as therapeutic alternatives to antibodies. Drug Discovery Today 9(12):525–529
33. Sato AK, Viswanathan M, Kent RB, Wood CR (2006) Therapeutic peptides: technological advances driving peptides into development. Curr Opin Biotechnol 17(6):638–642
34. Karimzadeh A, Hasanzadeh M, Shadjou N, de la Guardia M (2018) Peptide based biosensors. TrAC, Trends Anal Chem 107:1–20
35. Liu Q, Wang J, Boyd BJ (2015) Peptide-based biosensors. Talanta 136:114–127
36. Grant GA. Synthetic peptides: a user's guide. Oxford University Press on Demand; 2002.
37. Meloen R, Puijk W, Langeveld J, Langedijk J, Timmerman P (2003) Design of synthetic peptides for diagnostics. Curr Protein Pept Sci 4(4):253–260
38. Eissa S, Zourob M (2020) Ultrasensitive peptide-based multiplexed electrochemical biosensor for the simultaneous detection of Listeria monocytogenes and Staphylococcus aureus. Microchim Acta 187(9):486. https://doi.org/10.1007/s00604-020-04423-3
39. Eissa S, Zourob M (2020) A dual electrochemical/colorimetric magnetic nanoparticle/peptide-based platform for the detection of Staphylococcus aureus. Analyst 145(13):4606–4614. https://doi.org/10.1039/D0AN00673D
40. Zhao J, Wang S, Zhang S, Zhao P, Wang J, Yan M et al (2020) Peptide cleavage-mediated photoelectrochemical signal on-off via CuS electronic extinguisher for PSA detection. Biosens Bioelectron 150:111958. https://doi.org/10.1016/j.bios.2019.111958
41. Deng D, Hao Y, Yang S, Han Q, Liu L, Xiang Y et al (2019) A signal-on electrochemical biosensor for evaluation of caspase-3 activity and cell apoptosis by the generation of molecular electrocatalysts on graphene electrode surface for water oxidation. Sens Actuators, B Chem 286:415–420. https://doi.org/10.1016/j.snb.2019.01.137
42. Yogeswaran U, Kumar SA, Chen SM (2009) Nanostructured materials for electrochemical biosensors. Nova Science Publishers
43. Cosnier S (2015) Electrochemical Biosensors. Jenny Stanford Publishing
44. Negahdary M, Heli H (2019) An electrochemical peptide-based biosensor for the Alzheimer biomarker amyloid-β(1–42) using a microporous gold nanostructure. Microchim Acta 186(12):766. https://doi.org/10.1007/s00604-019-3903-x
45. Negahdary M, Sattarahmady N, Heli H (2020) Advances in prostate specific antigen biosensors-impact of nanotechnology. Clin Chim Acta 504:43–55. https://doi.org/10.1016/j.cca.2020.01.028
46. Huang X, Zhu Y, Kianfar E (2021) Nano biosensors: properties, applications and electrochemical techniques. Journal of Materials Research and Technology
47. Antiochia R (2020) Nanobiosensors as new diagnostic tools for SARS, MERS and COVID-19: from past to perspectives. Microchim Acta 187(12):1–13
48. Pumera M, Sanchez S, Ichinose I, Tang J (2007) Electrochemical nanobiosensors. Sens Actuators, B Chem 123(2):1195–1205
49. Parolo C, Merkoçi A (2013) Paper-based nanobiosensors for diagnostics. Chem Soc Rev 42(2):450–457. https://doi.org/10.1039/C2CS35255A
50. Gogotsi Y (2006) Nanomaterials handbook. CRC press
51. Wang J (2005) Nanomaterial-based electrochemical biosensors. Analyst 130(4):421–426
52. Pandey P, Datta M, Malhotra B (2008) Prospects of nanomaterials in biosensors. Anal Lett 41(2):159–209
53. Puiu M, Bala C (2018) Building switchable peptide-architectures on gold/composite surfaces: new perspectives in electrochemical bioassays. Curr Opin Electrochem 12:13–20
54. Bhattarai P, Hameed S (2020) Basics of biosensors and nanobiosensors. Nanobiosensors: From Design to Applications. 1–22
55. Ivnitski D, Abdel-Hamid I, Atanasov P, Wilkins E, Stricker S (2000) Application of electrochemical biosensors for detection of food pathogenic bacteria. Electroanalysis: An International Journal Devoted to Fundamental and Practical Aspects of Electroanalysis. 12(5):317–25.
56. Mayeux R (2004) Biomarkers: potential uses and limitations. NeuroRx 1(2):182–188
57. Aronson JK, Ferner RE (2017) Biomarkers—a general review. Current protocols in pharmacology. 76(1):9.23. 1–9.17.

58. Yuan L, Liu L (2021) Peptide-based electrochemical biosensing. Sens Actuators, B Chem 344:130232. https://doi.org/10.1016/j.snb.2021.130232
59. Vanova V, Mitrevska K, Milosavljevic V, Hynek D, Richtera L, Adam V (2021) Peptide-based electrochemical biosensors utilized for protein detection. Biosens Bioelectron 180:113087. https://doi.org/10.1016/j.bios.2021.113087
60. Barbosa AJ, Oliveira AR, Roque AC (2018) Protein-and peptide-based biosensors in artificial olfaction. Trends Biotechnol 36(12):1244–1258
61. Staderini M, González-Fernández E, Murray AF, Mount AR, Bradley M (2018) A tripod anchor offers improved robustness of peptide-based electrochemical biosensors. Sens Actuators, B Chem 274:662–667
62. Puiu M, Bala C (2018) Peptide-based biosensors: from self-assembled interfaces to molecular probes in electrochemical assays. Bioelectrochemistry 120:66–75
63. Tertis M, Hosu O, Feier B, Cernat A, Florea A, Cristea C (2021) Electrochemical peptide-based sensors for foodborne pathogens detection. Molecules 26(11):3200
64. Puiu M, Bala C (2019) Peptide-based electrochemical biosensors. Electrochemical Biosensors. Elsevier; 277–306
65. Microbiology ASf (2007) Applied and environmental microbiology. 73, no. 23. American Society for Microbiology
66. Johnson EA (2019) Clostridium botulinum. Food microbiology: fundamentals and frontiers. 487–512.
67. Caratelli V, Fillo S, D'Amore N, Rossetto O, Pirazzini M, Moccia M et al (2021) Paper-based electrochemical peptide sensor for on-site detection of botulinum neurotoxin serotype A and C. Biosens Bioelectron 183:113210. https://doi.org/10.1016/j.bios.2021.113210
68. Heitman J, Howlett BJ, Crous PW, Stukenbrock EH, James TY, Gow NAR. The Fungal Kingdom. Wiley; 2017.
69. Lee IH, Zhao C, Cho Y, Harwig SSL, Cooper EL, Lehrer RI (1997) Clavanins, α-helical antimicrobial peptides from tunicate hemocytes. FEBS Lett 400(2):158–162. https://doi.org/10.1016/S0014-5793(96)01374-9
70. Ribeiro KL, Frías IAM, Silva AG, Lima-Neto RG, Sá SR, Franco OL et al (2021) Impedimetric clavmo peptide-based sensor differentiates ploidy of candida species. Biochem Eng J 167:107918. https://doi.org/10.1016/j.bej.2020.107918
71. Tasaki Y, Inoue N, Shimizu M, Sugimoto N, Ishikawa S, Mizuta M et al (2021) Serum insulin-like growth factor-binding protein 2 levels as an indicator for disease severity in enterohemorrhagic Escherichia coli induced hemolytic uremic syndrome. Ren Fail 43(1):382–387
72. Ropero-Vega JL, Redondo-Ortega JF, Galvis-Curubo YJ, Rondón-Villarreal P, Flórez-Castillo JM (2021) A Bioinspired peptide in TIR protein as recognition molecule on electrochemical biosensors for the detection of E. coli O157:H7 in an aqueous matrix. Molecules. 26(9):2559
73. Singh SK, Ruzek D (2020) Neuroviral infections: two volume set. CRC Press
74. Baek SH, Park CY, Nguyen TP, Kim MW, Park JP, Choi C et al (2020) Novel peptides functionalized gold nanoparticles decorated tungsten disulfide nanoflowers as the electrochemical sensing platforms for the norovirus in an oyster. Food Control 114:107225. https://doi.org/10.1016/j.foodcont.2020.107225
75. Chan C-Y, Guo J, Sun C, Tsang M-K, Tian F, Hao J et al (2015) A reduced graphene oxide-Au based electrochemical biosensor for ultrasensitive detection of enzymatic activity of botulinum neurotoxin A. Sens Actuators, B Chem 220:131–137. https://doi.org/10.1016/j.snb.2015.05.052
76. Yan J, Shi Q, You K, Li Y, He Q (2019) Phage displayed mimotope peptide-based immunosensor for green and ultrasensitive detection of mycotoxin deoxynivalenol. J Pharm Biomed Anal 168:94–101. https://doi.org/10.1016/j.jpba.2019.01.051
77. Chen Y, Zhang S, Hong Z, Lin Y, Dai H (2019) A mimotope peptide-based dual-signal readout competitive enzyme-linked immunoassay for non-toxic detection of zearalenone. Journal of Materials Chemistry B 7(44):6972–6980. https://doi.org/10.1039/C9TB01167F
78. Liberato MS, Mancini RSN, Factori IM, Ferreira FF, de Oliveira VL, Carnielli JBT et al (2019) Peptide-based assemblies on electrospun polyamide-6/chitosan nanofibers for detecting visceral leishmaniasis antibodies. ACS Appl Electron Mater 1(10):2086–2095. https://doi.org/10.1021/acsaelm.9b00476
79. de Miranda JL, Oliveira MDL, Oliveira IS, Frias IAM, Franco OL, Andrade CAS (2017) A simple nanostructured biosensor based on clavanin A antimicrobial peptide for gram-negative bacteria detection. Biochem Eng J 124:108–114. https://doi.org/10.1016/j.bej.2017.04.013
80. Laronha H, Caldeira J (2020) Structure and function of human matrix metalloproteinases. Cells 9(5):1076
81. Liao H-Y, Da C-M, Liao B, Zhang H-H (2021) Roles of matrix metalloproteinase-7 (MMP-7) in cancer. Clin Biochem 92:9–18. https://doi.org/10.1016/j.clinbiochem.2021.03.003
82. Cheng W, Ma J, Kong D, Zhang Z, Khan A, Yi C et al (2021) One step electrochemical detection for matrix metalloproteinase 2 based on anodic stripping of silver nanoparticles mediated by host-guest interactions. Sens Actuators, B Chem 330:129379. https://doi.org/10.1016/j.snb.2020.129379
83. Xi X, Wen M, Song S, Zhu J, Wen W, Zhang X et al (2020) A H2O2-free electrochemical peptide biosensor based on Au@Pt bimetallic nanorods for highly sensitive sensing of matrix metalloproteinase 2. Chem Commun 56(45):6039–6042. https://doi.org/10.1039/D0CC01598A
84. Ye Z, Li G, Xu L, Yu Q, Yue X, Wu Y et al (2020) Peptide-conjugated hemin/G-quadruplex as a versatile probe for "signal-on" electrochemical peptide biosensor. Talanta 209:120611. https://doi.org/10.1016/j.talanta.2019.120611
85. Zheng J, Zhao H, Ning G, Sun W, Wang L, Liang H et al (2021) A novel affinity peptide–antibody sandwich electrochemical biosensor for PSA based on the signal amplification of MnO2-functionalized covalent organic framework. Talanta 233:122520. https://doi.org/10.1016/j.talanta.2021.122520
86. Lakhi N, Moretti M (2016) Alpha-fetoprotein: functions and clinical application. Nova Science Publishers, Incorporated
87. Zhao S, Liu N, Wang W, Xu Z, Wu Y, Luo X (2021) An electrochemical biosensor for alpha-fetoprotein detection in human serum based on peptides containing isomer D-Amino acids with enhanced stability and antifouling property. Biosensors and Bioelectronics. 190:113466
88. Garzon R, Calin GA, Croce CM (2009) MicroRNAs in cancer. Annu Rev Med 60:167–179
89. Bolat G, Akbal Vural O, Tugce Yaman Y, Abaci S (2021) Label-free impedimetric miRNA-192 genosensor platform using graphene oxide decorated peptide nanotubes composite. Microchem J 166:106218. https://doi.org/10.1016/j.microc.2021.106218
90. Hamley IW (2014) Peptide nanotubes. Angew Chem Int Ed 53(27):6866–6881
91. Yaman YT, Vural OA, Bolat G, Abaci S (2020) One-pot synthesized gold nanoparticle-peptide nanotube modified disposable sensor for impedimetric recognition of miRNA 410. Sens Actuators, B Chem 320:128343. https://doi.org/10.1016/j.snb.2020.128343
92. Wang H, Yuan Y, Chai Y, Yuan R (2015) Sandwiched electrochemiluminescent peptide biosensor for the detection of prognostic indicator in early-stage cancer based on hollow, magnetic, and self-enhanced nanosheets. Small 11(30):3703–3709. https://doi.org/10.1002/smll.201500321

93. Tang Y, Dai Y, Huang X, Li L, Han B, Cao Y et al (2019) Self-assembling peptide-based multifunctional nanofibers for electrochemical identification of breast cancer stem-like cells. Anal Chem 91(12):7531–7537. https://doi.org/10.1021/acs.analchem.8b05359
94. Lian M, Chen X, Liu X, Yi Z, Yang W (2017) A self-assembled peptide nanotube–chitosan composite as a novel platform for electrochemical cytosensing. Sens Actuators, B Chem 251:86–92. https://doi.org/10.1016/j.snb.2017.04.102
95. Wu R, Fan G-C, Jiang L-P, Zhu J-J (2018) Peptide-based photoelectrochemical cytosensor using a hollow-TiO2/EG/ZnIn2S4 cosensitized structure for ultrasensitive detection of early apoptotic cells and drug evaluation. ACS Appl Mater Interfaces 10(5):4429–4438. https://doi.org/10.1021/acsami.7b16054
96. Zheng X, Li L, Cui K, Zhang Y, Zhang L, Ge S et al (2018) Ultrasensitive enzyme-free biosensor by coupling cyclodextrin functionalized Au nanoparticles and high-performance Au-paper electrode. ACS Appl Mater Interfaces 10(4):3333–3340. https://doi.org/10.1021/acsami.7b17037
97. Meng F, Sun H, Huang Y, Tang Y, Chen Q, Miao P (2019) Peptide cleavage-based electrochemical biosensor coupling graphene oxide and silver nanoparticles. Anal Chim Acta 1047:45–51. https://doi.org/10.1016/j.aca.2018.09.053
98. Vural T, Yaman YT, Ozturk S, Abaci S, Denkbas EB (2018) Electrochemical immunoassay for detection of prostate specific antigen based on peptide nanotube-gold nanoparticle-polyaniline immobilized pencil graphite electrode. J Colloid Interface Sci 510:318–326. https://doi.org/10.1016/j.jcis.2017.09.079
99. Parnsubsakul A, Safitri RE, Rijiravanich P, Surareungchai W (2017) Electrochemical assay of proteolytically active prostate specific antigen based on anodic stripping voltammetry of silver enhanced gold nanoparticle labels. J Electroanal Chem 785:125–130. https://doi.org/10.1016/j.jelechem.2016.12.010
100. Xia N, Deng D, Yang S, Hao Y, Wang L, Liu Y et al (2019) Electrochemical immunosensors with protease as the signal label for the generation of peptide-Cu(II) complexes as the electrocatalysts toward water oxidation. Sens Actuators, B Chem 291:113–119. https://doi.org/10.1016/j.snb.2019.04.063
101. Xie S, Zhang J, Yuan Y, Chai Y, Yuan R (2015) An electrochemical peptide cleavage-based biosensor for prostate specific antigen detection via host–guest interaction between ferrocene and β-cyclodextrin. Chem Commun 51(16):3387–3390. https://doi.org/10.1039/C4CC10363G
102. He Y, Xie S, Yang X, Yuan R, Chai Y (2015) Electrochemical peptide biosensor based on in situ silver deposition for detection of prostate specific antigen. ACS Appl Mater Interfaces 7(24):13360–13366. https://doi.org/10.1021/acsami.5b01827
103. Wang Y, Qu Y, Liu G, Hou X, Huang Y, Wu W et al (2015) Electrochemical immunoassay for the prostate specific antigen using a reduced graphene oxide functionalized with a high molecular-weight silk peptide. Microchim Acta 182(11):2061–2067. https://doi.org/10.1007/s00604-015-1552-2
104. Wang D, Zheng Y, Chai Y, Yuan Y, Yuan R (2015) Target protein induced cleavage of a specific peptide for prostate-specific antigen detection with positively charged gold nanoparticles as signal enhancer. Chem Commun 51(52):10521–10523. https://doi.org/10.1039/C5CC02148K
105. Tang Z, Fu Y, Ma Z (2017) Bovine serum albumin as an effective sensitivity enhancer for peptide-based amperometric biosensor for ultrasensitive detection of prostate specific antigen. Biosens Bioelectron 94:394–399. https://doi.org/10.1016/j.bios.2017.03.030
106. Yu Q, Wu Y, Liu Z, Lei S, Li G, Ye B (2018) Novel electrochemical biosensor based on cationic peptide modified hemin/G-quadruples enhanced peroxidase-like activity. Biosens Bioelectron 107:178–183. https://doi.org/10.1016/j.bios.2018.02.014
107. Ding C, Wang X, Luo X (2019) Dual-mode electrochemical assay of prostate-specific antigen based on antifouling peptides functionalized with electrochemical probes and internal references. Anal Chem 91(24):15846–15852. https://doi.org/10.1021/acs.analchem.9b04206
108. Wang D, Chai Y, Yuan Y, Yuan R (2017) A peptide cleavage-based ultrasensitive electrochemical biosensor with an ingenious two-stage DNA template for highly efficient DNA exponential amplification. Anal Chem 89(17):8951–8956
109. Kou B-B, Zhang L, Xie H, Wang D, Yuan Y-L, Chai Y-Q et al (2016) DNA enzyme-decorated DNA nanoladders as enhancer for peptide cleavage-based electrochemical biosensor. ACS Appl Mater Interfaces 8(35):22869–22874. https://doi.org/10.1021/acsami.6b07017
110. Wei Z, Wang H, Ma Z, Han H (2018) Amperometric biosensor of matrix metalloproteinase-7 enhanced by Pd-functionalized carbon nanocomposites. Nanoscale Res Lett 13(1):375. https://doi.org/10.1186/s11671-018-2793-x
111. Zheng Y, Ma Z (2018) Dual-reaction triggered sensitivity amplification for ultrasensitive peptide-cleavage based electrochemical detection of matrix metalloproteinase-7. Biosens Bioelectron 108:46–52. https://doi.org/10.1016/j.bios.2018.02.045
112. Wang H, Ma Z (2018) A novel strategy for improving amperometric biosensor sensitivity using dual-signal synergistic effect for ultrasensitive detection of matrix metalloproteinase-2. Sens Actuators, B Chem 266:46–51
113. Jing P, Yi H, Xue S, Yuan R, Xu W (2015) A 'signal on-off' electrochemical peptide biosensor for matrix metalloproteinase 2 based on target induced cleavage of a peptide. RSC Adv 5(81):65725–65730. https://doi.org/10.1039/C5RA10662A
114. Wang H, Ma Z, Han H (2019) A novel impedance enhancer for amperometric biosensor based ultrasensitive detection of matrix metalloproteinase-2. Bioelectrochemistry 130:107324. https://doi.org/10.1016/j.bioelechem.2019.06.009
115. Wang D, Yuan Y, Zheng Y, Chai Y, Yuan R (2016) An electrochemical peptide cleavage-based biosensor for matrix metalloproteinase-2 detection with exonuclease III-assisted cycling signal amplification. Chem Commun 52(35):5943–5945. https://doi.org/10.1039/C6CC00928J
116. Xu W, Jing P, Yi H, Xue S, Yuan R (2016) Bimetallic Pt/Pd encapsulated mesoporous-hollow CeO2 nanospheres for signal amplification toward electrochemical peptide-based biosensing for matrix metalloproteinase 2. Sens Actuators, B Chem 230:345–352. https://doi.org/10.1016/j.snb.2016.02.064
117. Liu X, Wang Q, Chen J, Chen X, Yang W (2021) Ultrasensitive electrochemiluminescence biosensor for the detection of tumor exosomes based on peptide recognition and luminol-AuNPs@g-C3N4 nanoprobe signal amplification. Talanta 221:121379. https://doi.org/10.1016/j.talanta.2020.121379
118. Pegtel DM, Gould SJ (2019) Exosomes. Annu Rev Biochem 88(1):487–514. https://doi.org/10.1146/annurev-biochem-013118-111902
119. Chen M, Song Z, Han R, Li Y, Luo X (2021) Low fouling electrochemical biosensors based on designed Y-shaped peptides with antifouling and recognizing branches for the detection of IgG in human serum. Biosens Bioelectron 178:113016. https://doi.org/10.1016/j.bios.2021.113016
120. Klein MO, Battagello DS, Cardoso AR, Hauser DN, Bittencourt JC, Correa RG (2019) Dopamine: functions, signaling, and association with neurological diseases. Cell Mol Neurobiol 39(1):31–59
121. Wang W, Han R, Tang K, Zhao S, Ding C, Luo X (2021) Biocompatible peptide hydrogels with excellent antibacterial and catalytic properties for electrochemical sensing application. Anal Chim Acta 1154:338295. https://doi.org/10.1016/j.aca.2021.338295

122. Panza F, Lozupone M, Logroscino G, Imbimbo BP (2019) A critical appraisal of amyloid-β-targeting therapies for Alzheimer disease. Nat Rev Neurol 15(2):73–88
123. Reichlin T, Hochholzer W, Bassetti S, Steuer S, Stelzig C, Hartwiger S et al (2009) Early diagnosis of myocardial infarction with sensitive cardiac troponin assays. N Engl J Med 361(9):858–867
124. Coiffier B (2007) Rituximab therapy in malignant lymphoma. Oncogene 26(25):3603–3613
125. Huang S, Tang R, Zhang T, Zhao J, Jiang Z, Wang Q (2021) Anti-fouling poly adenine coating combined with highly specific CD20 epitope mimetic peptide for rituximab detection in clinical patients' plasma. Biosens Bioelectron 171:112678. https://doi.org/10.1016/j.bios.2020.112678
126. Weaver K (2012) Trypsin: structure, biosynthesis and functions. Nova Science Publishers, Incorporated
127. Song X, Zhao L, Luo C, Ren X, Yang L, Wei Q (2021) Peptide-based biosensor with a luminescent copper-based metal–organic framework as an electrochemiluminescence emitter for trypsin assay. Anal Chem 93(28):9704–9710. https://doi.org/10.1021/acs.analchem.1c00850
128. Stromberg LR. Detection methods for lipopolysaccharides: past and present. IntechOpen; 2017.
129. Yang L, Gao Y, Fang K, Sun H, Sun J, Liu H et al (2020) Photocatalytically renewable peptide-based electrochemical impedance method for sensing lipopolysaccharide. Microchim Acta 187(6):349. https://doi.org/10.1007/s00604-020-04321-8
130. Farag AK, Roh EJ (2019) Death-associated protein kinase (DAPK) family modulators: current and future therapeutic outcomes. Med Res Rev 39(1):349–385
131. Xiao K, Meng L, Du C, Zhang Q, Yu Q, Zhang X et al (2021) A label-free photoelectrochemical biosensor with near-zero-background noise for protein kinase A activity assay based on porous ZrO2/CdS octahedra. Sens Actuators, B Chem 328:129096. https://doi.org/10.1016/j.snb.2020.129096
132. Fan X, Li Z, Wang S, Liu L, Liu P, Chen F et al (2019) Electrochemical Impedance biosensor for the determination of lipopolysaccharide using peptide as the recognition molecule. J Braz Chem Soc 30:1762–1768
133. Fan X, Li Z, Wang S, Wang Y, Yu L, Fan X (2020) An electrochemiluminescence sandwich biosensor for the detection of lipopolysaccharide. Quim Nova 43:747–751
134. Zhang K, Yang Q, Fan Z, Zhao J, Li H. Platelet-driven formation of interface peptide nano-network biosensor enabling a non-invasive means for early detection of Alzheimer's disease. Biosensors and Bioelectronics. 2019;145:111701.
135. Xing Y, Feng X-Z, Zhang L, Hou J, Han G-C, Chen Z (2017) A sensitive and selective electrochemical biosensor for the determination of beta-amyloid oligomer by inhibiting the peptide-triggered in situ assembly of silver nanoparticles. Int J Nanomedicine 12:3171–3179. https://doi.org/10.2147/IJN.S132776
136. Sun L, Zhong Y, Gui J, Wang X, Zhuang X, Weng J (2018) A hydrogel biosensor for high selective and sensitive detection of amyloid-beta oligomers. Int J Nanomedicine 13:843–856. https://doi.org/10.2147/IJN.S152163
137. Xia N, Wang X, Yu J, Wu Y, Cheng S, Xing Y et al (2017) Design of electrochemical biosensors with peptide probes as the receptors of targets and the inducers of gold nanoparticles assembly on electrode surface. Sens Actuators, B Chem 239:834–840. https://doi.org/10.1016/j.snb.2016.08.079
138. Xia N, Chen Z, Liu Y, Ren H, Liu L (2017) Peptide aptamer-based biosensor for the detection of human chorionic gonadotropin by converting silver nanoparticles-based colorimetric assay into sensitive electrochemical analysis. Sens Actuators, B Chem 243:784–791. https://doi.org/10.1016/j.snb.2016.12.066
139. Gu S, Shi X-M, Zhang D, Fan G-C, Luo X (2021) Peptide-based photocathodic biosensors: integrating a recognition peptide with an antifouling peptide. Anal Chem 93(4):2706–2712
140. Allafchian AR, Moini E, Mirahmadi-Zare SZ (2018) Flower-like self-assembly of diphenylalanine for electrochemical human growth hormone biosensor. IEEE Sens J 18(21):8979–8985
141. Wang G, Han R, Su X, Li Y, Xu G, Luo X (2017) Zwitterionic peptide anchored to conducting polymer PEDOT for the development of antifouling and ultrasensitive electrochemical DNA sensor. Biosens Bioelectron 92:396–401. https://doi.org/10.1016/j.bios.2016.10.088
142. Lian M, Chen X, Lu Y, Yang W (2016) Self-assembled peptide hydrogel as a smart biointerface for enzyme-based electrochemical biosensing and cell monitoring. ACS Appl Mater Interfaces 8(38):25036–25042. https://doi.org/10.1021/acsami.6b05409
143. Komori K, Terse-Thakoor T, Mulchandani A (2015) Bioelectrochemistry of heme peptide at seamless three-dimensional carbon nanotubes/graphene hybrid films for highly sensitive electrochemical biosensing. ACS Appl Mater Interfaces 7(6):3647–3654. https://doi.org/10.1021/am508032p
144. Pang Y, Zhang Q, Sun X, Ji J, Pi F, Shen X (2018) Self-assembled diphenylalanine peptide fibrils with ultra-high aspect ratio: a platform for sensitive electrochemical H2O2 sensor. Int J Electrochem Sci 13:8518–8529
145. Wang Y, Cui M, Jiao M, Luo X (2018) Antifouling and ultrasensitive biosensing interface based on self-assembled peptide and aptamer on macroporous gold for electrochemical detection of immunoglobulin E in serum. Anal Bioanal Chem 410(23):5871–5878. https://doi.org/10.1007/s00216-018-1201-9
146. Lei Y-M, Zhou J, Chai Y-Q, Zhuo Y, Yuan R (2018) SnS2 Quantum dots as new emitters with strong electrochemiluminescence for ultrasensitive antibody detection. Anal Chem 90(20):12270–12277. https://doi.org/10.1021/acs.analchem.8b03623
147. Biyani M, Kawai K, Kitamura K, Chikae M, Biyani M, Ushijima H et al (2016) PEP-on-DEP: a competitive peptide-based disposable electrochemical aptasensor for renin diagnostics. Biosens Bioelectron 84:120–125. https://doi.org/10.1016/j.bios.2015.12.078
148. Han K, Li G, Tian L, Li L, Shi Y, Huang T et al (2021) Multifunctional peptide-oligonucleotide conjugate promoted sensitive electrochemical biosensing of cardiac troponin I. Biochem Eng J 174:108104. https://doi.org/10.1016/j.bej.2021.108104
149. Dong M, Li M, Qi H, Li Z, Gao Q, Zhang C (2015) Electrogenerated chemiluminescence peptide-based biosensing method for cardiac troponin I using peptide-integrating Ru(bpy)32+-functionalized gold nanoparticles as nanoprobe. Gold Bulletin 48(1):21–29. https://doi.org/10.1007/s13404-015-0156-2
150. Wang B, Jing R, Qi H, Gao Q, Zhang C (2016) Label-free electrochemical impedance peptide-based biosensor for the detection of cardiac troponin I incorporating gold nanoparticles modified carbon electrode. J Electroanal Chem 781:212–217. https://doi.org/10.1016/j.jelechem.2016.08.005
151. Lin Y, Shen R, Liu N, Yi H, Dai H, Lin J (2018) A highly sensitive peptide-based biosensor using NiCo2O4 nanosheets and g-C3N4 nanocomposite to construct amplified strategy for trypsin detection. Anal Chim Acta 1035:175–183. https://doi.org/10.1016/j.aca.2018.06.040
152. Zhou Y, Yin H, Li X, Li Z, Ai S, Lin H (2016) Electrochemical biosensor for protein kinase A activity assay based on gold nanoparticles-carbon nanospheres, phos-tag-biotin and β-galactosidase. Biosens Bioelectron 86:508–515. https://doi.org/10.1016/j.bios.2016.07.004
153. Yin H, Wang M, Li B, Yang Z, Zhou Y, Ai S (2015) A sensitive electrochemical biosensor for detection of protein kinase A activity and inhibitors based on Phos-tag and enzymatic signal

amplification. Biosens Bioelectron 63:26–32. https://doi.org/10.1016/j.bios.2014.07.016
154. Wang Y, Li X, Waterhouse GIN, Zhou Y, Yin H, Ai S (2019) Photoelectrochemical biosensor for protein kinase A detection based on carbon microspheres, peptide functionalized Au-ZIF-8 and TiO2/g-C3N4. Talanta 196:197–203. https://doi.org/10.1016/j.talanta.2018.12.035
155. Sun K, Chang Y, Zhou B, Wang X, Liu L (2017) Gold nanoparticles-based electrochemical method for the detection of protein kinase with a peptide-like inhibitor as the bioreceptor. Int J Nanomedicine 12:1905–1915. https://doi.org/10.2147/IJN.S127957
156. Li W, Li H, Wu S, Feng C, Li G (2016) Highly sensitive protein detection based on DNAzyme cycling activated surface assembly of peptide decorated nanoparticles. Electrochem Commun 71:84–88. https://doi.org/10.1016/j.elecom.2016.08.011
157. Wu Y, Zou L, Lei S, Yu Q, Ye B (2017) Highly sensitive electrochemical thrombin aptasensor based on peptide-enhanced electrocatalysis of hemin/G-quadruplex and nanocomposite as nanocarrier. Biosens Bioelectron 97:317–324. https://doi.org/10.1016/j.bios.2017.06.023
158. Song S, Hu X, Li H, Zhao J, Koh K, Chen H (2018) Guests involved CB[8] capped silver nanoparticles as a means of electrochemical signal enhancement for sensitive detection of Caspase-3. Sens Actuators, B Chem 274:54–59. https://doi.org/10.1016/j.snb.2018.07.143
159. Khalilzadeh B, Shadjou N, Afsharan H, Eskandani M, Nozad Charoudeh H, Rashidi M-R (2016) Reduced graphene oxide decorated with gold nanoparticle as signal amplification element on ultra-sensitive electrochemiluminescence determination of caspase-3 activity and apoptosis using peptide based biosensor. Bioimpacts 6(3):135–147. https://doi.org/10.15171/bi.2016.20
160. Khalilzadeh B, Charoudeh HN, Shadjou N, Mohammad-Rezaei R, Omidi Y, Velaei K et al (2016) Ultrasensitive caspase-3 activity detection using an electrochemical biosensor engineered by gold nanoparticle functionalized MCM-41: Its application during stem cell differentiation. Sens Actuators, B Chem 231:561–575. https://doi.org/10.1016/j.snb.2016.03.043
161. Wang Z, Xu E, Wang C, Wei W, Liu Y, Liu S (2019) High specificity and efficiency electrochemical detection of poly(ADP-ribose) polymerase-1 activity based on versatile peptide-templated copper nanoparticles and detection array. Anal Chim Acta 1091:95–102. https://doi.org/10.1016/j.aca.2019.09.023
162. Sewald N, Jakubke H-D (2015) Peptides: chemistry and biology. John Wiley & Sons